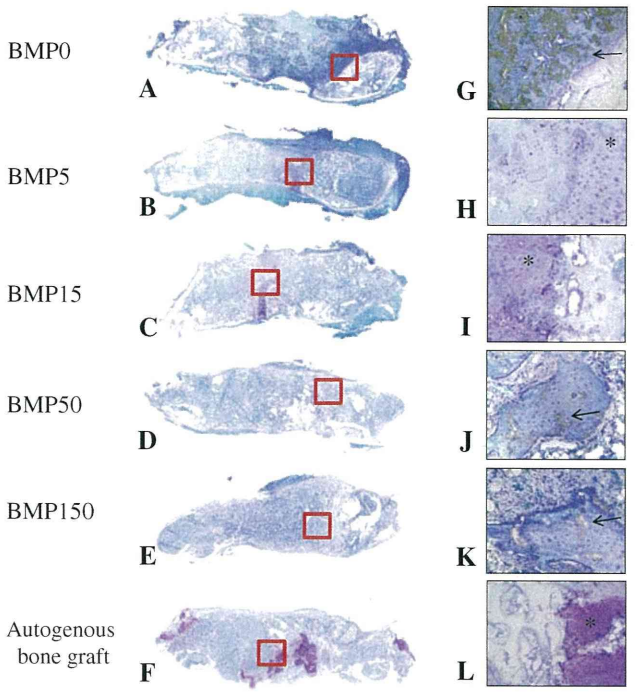

Fig. 4A–L Representative longitudinal histology sections of fusion mass of each group at 8 weeks after surgery are shown. (**A**) BMP0; (**B**) BMP5; (**C**) BMP15; (**D**) BMP50; (**E**) BMP150; (**F**) autogenous bone graft (Stain, Toluidine blue; original magnification, **A–F**: ×1). (**G**) BMP0; (**H**) BMP5; (**I**) BMP15; (**J**) BMP50; (**K**) BMP150; (**L**) autogenous bone graft (Metachromatic; original magnification ×100 for **G** and **L**, original magnification ×200 for **H**, **I**, **J** and **K**). Positive cartilage remnant in the fusion mass is not present in only section of groups of BMP50 and BMP150. More than 50 μg/side of E-BMP-2 treatment could histologically achieve lumbar spinal fusion as well as autogenous bone graft. Arrows indicate residual β-TCP.

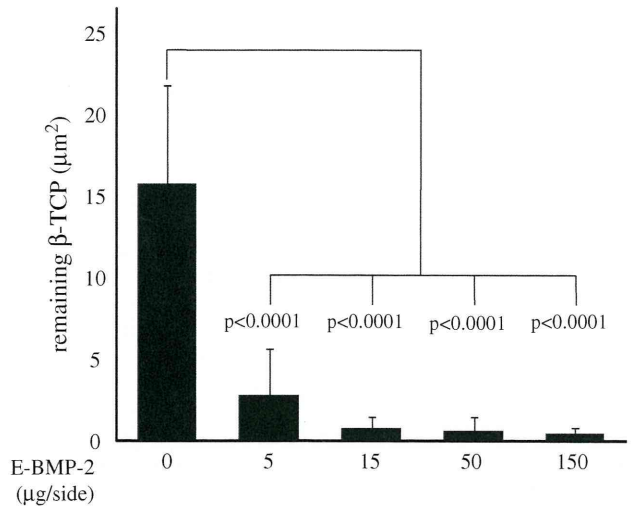

Fig. 5 Amounts of residual β-TCP were quantitatively assessed using bone histomorphometry software and expressed per square micron. Resorption of β-TCP was higher in the groups treated with E-BMP-2 than in the group treated without E-BMP-2. E-BMP-2 treatment could histologically achieve remodeling of newly formed fusion mass the same as autogenous bone graft. Values are mean ± SD.

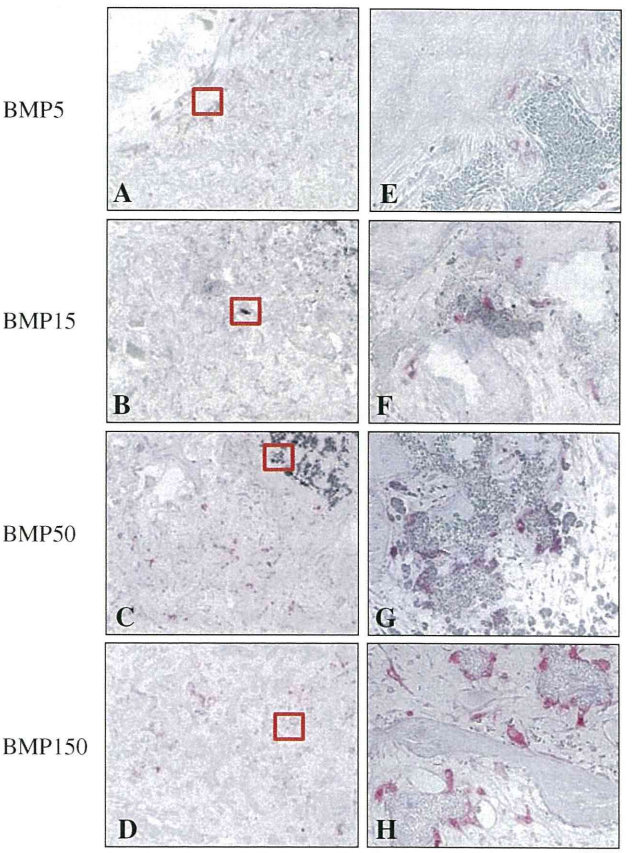

Fig. 6A–H Representative longitudinal histology sections of fusion mass of each group at 4 weeks after surgery are shown. (**A** and **E**) BMP5; (**B** and **F**) BMP15: (**C** and **G**) BMP50; (**D** and **H**) BMP150. (Stain, TRAP; original magnification, **A–D**: x100, **E–H**: ×400). Right panels show higher magnifications of each left panel. E-BMP-2 treatment could histologically achieve remodeling of newly formed fusion mass as same as autogenous bone graft. TRAP-positive giant cells, that are osteoclasts, are abundant in the BMP50 and BMP150 groups.

followup of 3D-CT, different results might have been obtained at later stages. Third, our sample size in each group was not sufficient to yield substantial effects and the study is likely underpowered; we therefore consider the study preliminary. On the other hand, we previously found E-BMP-2 has osteoinductive activity equivalent to that currently produced in BMP-2 gene-transfected animal cells (Chinese hamster ovary cells) [45]. However, it is essential to evaluate the safety of E-BMP-2 for clinical use. In several previous studies using E-BMP-2 [18, 29, 45], its safety was not sufficiently examined. Evaluation of the safety of E-BMP-2 is required in preclinical studies.

One problem with wide clinical use of BMPs is their high cost of production, since they are originally derived from mammalian CHO cells [42]. To address this issue, Sebald et al. devised a novel method to produce rhBMP-2 derived from E. coli and convert BMP monomers to biologically active dimers (E-BMP-2) [18, 29]. E-BMP-2 has

osteoinductive activity the same as CHO-derived rhBMP-2 both in vivo and in vitro [45]. However, these reports included only results for E-BMP-2-induced ectopic bone formation. Our question in this study was whether E-BMP-2-adsorbed β-TCP can achieve lumbar spinal fusion in a rabbit model the same as autogenous bone graft. Our findings suggest E-BMP-2-adsorbed β-TCP granules can effectively achieve posterolateral spinal fusion in a rabbit model the same as autogenous bone graft. On the other hand, from the original phase of preclinical and clinical application of BMPs, they have been locally delivered with Type I collagen sponges [5, 6, 10]. Although it is now possible to generate large amounts of recombinant human BMPs for medical use, the major challenge remains in the development of optimal local delivery systems for these proteins. To address this issue, we have investigated a biodegradable polymer as a carrier for BMPs yielding slow release and increasing the effects of BMPs [30], while Seeherman et al. have investigated the efficacy of calcium phosphate paste as a carrier for rhBMP-2 for the treatment of osteotomy [35]. We have generated an osteoinductive composite consisting of rhBMP-2, β-TCP powder, and biodegradable polymer for the treatment of various skeletal disorder models [12, 26, 36]. However, the results of these investigations are not yet clinically applicable because of the use of agents not approved for clinical use, such as biodegradable polymers. To address this problem, we used β-TCP, which is widely applied clinically, as a delivery system for BMP. As a result the necessary amount of BMP-2 to obtain lumbar spinal fusion is higher than that reported in our previous study [26]. We found lumbar spinal fusion occurred with the use of β-TCP and extended release of E-BMP-2 as previously described [32, 43]. Large quantities of BMPs facilitated osteoclast formation and resultant resorption and remodeling of newly formed bone in a dose-dependent manner (Figs. 5, 6), as previously reported [36]. This excessive osteoclast differentiation and bone resorption is an indirect effect of osteoblast differentiation and RANKL (receptor activator of NFκB ligand) expression induced by BMP stimulation [28, 37, 46] and a direct effect of BMP on osteoclastogenesis [44]. As previously described [21], these observations also indicate that excessive amounts of BMP might fail to yield required new bone formation, and that it is important to use optimal doses of BMP in clinical situations such as spinal fusion. E-BMP-2-adsorbed β-TCP granules may thus be useful as new materials for osteogenesis, especially for spinal fusion, and successfully address issues related to the clinical application of BMPs noted above.

Our preliminary findings suggest E-BMP-2-adsorbed porous β-TCP could be an effective alternative to autogenous bone grafting for generation of new bone and promotion of regenerative repair of bone, and potentially utilizable in the clinical setting for the treatment of spinal disorders.

Acknowledgments We thank Drs. A. Suzuki, K. Yano, T. Matsumoto, H. Yasuda, K. Sugama, H. Irie, and A. Yamada, W. Fukushima, M Fukui, and also Ms. A. Inagaki, Ms. K. Hata, Ms. K. Kamei, and Ms. Y. Hanamoto for technical and statistical assistance. E-BMP-2 was produced and kindly provided by Dr. W. Sebald (Würzburg, Germany) and donated to us through Osteopharma Inc. (Osaka, Japan). The β-TCP granules were donated by HOYA Corp. (Tokyo, Japan).

References

1. Akamaru T, Suh D, Boden SD, Kim HS, Minamide A, Louis-Ugbo J. Simple carrier matrix modifications can enhance delivery of recombinant human bone morphogenetic protein-2 for posterolateral spine fusion. *Spine*. 2003;28:429–434.
2. Allen RT, Lee YP, Stimson E, Garfin SR. Bone morphogenetic protein-2 (BMP-2) in the treatment of pyogenic vertebral osteomyelitis. *Spine*. 2007;32:2996–3006.
3. Arosarena OA, Collins WL. Bone regeneration in the rat mandible with bone morphogenetic protein-2: a comparison of two carriers. *Otolaryngol Head Neck Surg*. 2005;132:592–597.
4. Arrington ED, Smith WJ, Chambers HG, Bucknell AL, Davino NA. Complications of iliac crest bone graft harvesting. *Clin Orthop Relat Res*. 1996;329:300–309.
5. Boden SD, Kang J, Sandhu H, Heller JG. Use of recombinant human bone morphogenetic protein-2 to achieve posterolateral lumbar spine fusion in humans: a prospective, randomized clinical pilot trial: 2002 Volvo Award in clinical studies. *Spine*. 2002;27:2662–2673.
6. Boden SD, Schimandle JH, Hutton WC. An experimental lumbar intertransverse process spinal fusion model. Radiographic, histologic, and biomechanical healing characteristics. *Spine*. 1995;20:412–420.
7. David SM, Gruber HE, Meyer RA, Jr., Murakami T, Tabor OB, Howard BA, Wozney JM, Hanley EN, Jr. Lumbar spinal fusion using recombinant human bone morphogenetic protein in the canine. A comparison of three dosages and two carriers. *Spine*. 1999;24:1973–1979.
8. Dimar JR, Glassman SD, Burkus KJ, Carreon LY. Clinical outcomes and fusion success at 2 years of single-level instrumented posterolateral fusions with recombinant human bone morphogenetic protein-2/compression resistant matrix versus iliac crest bone graft. *Spine*. 2006;31:2534–2539; discussion 2540.
9. Glassman SD, Dimar JR, 3rd, Burkus K, Hardacker JW, Pryor PW, Boden SD, Carreon LY. The efficacy of rhBMP-2 for posterolateral lumbar fusion in smokers. *Spine*. 2007;32:1693–1698.
10. Govender S, Csimma C, Genant HK, Valentin-Opran A, Amit Y, Arbel R, Aro H, Atar D, Bishay M, Borner MG, Chiron P, Choong P, Cinats J, Courtenay B, Feibel R, Geulette B, Gravel C, Haas N, Raschke M, Hammacher E, van der Velde D, Hardy P, Holt M, Josten C, Ketterl RL, Lindeque B, Lob G, Mathevon H, McCoy G, Marsh D, Miller R, Munting E, Oevre S, Nordsletten L, Patel A, Pohl A, Rennie W, Reynders P, Rommens PM, Rondia J, Rossouw WC, Daneel PJ, Ruff S, Ruter A, Santavirta S, Schildhauer TA, Gekle C, Schnettler R, Segal D, Seiler H, Snowdowne RB, Stapert J, Taglang G, Verdonk R, Vogels L, Weckbach A, Wentzensen A, Wisniewski T. Recombinant human bone morphogenetic protein-2 for treatment of open tibial fractures: a prospective, controlled, randomized study of four hundred and fifty patients. *J Bone Joint Surg Am*. 2002;84:2123–2134.

11. Grauer JN, Patel TC, Erulkar JS, Troiano NW, Panjabi MM, Friedlaender GE. 2000 Young Investigator Research Award winner. Evaluation of OP-1 as a graft substitute for intertransverse process lumbar fusion. *Spine.* 2001;26:127–133.
12. Hoshino M, Namikawa T, Kato M, Terai H, Taguchi S, Takaoka K. Repair of bone defects in revision hip arthroplasty by implantation of a new bone-inducing material comprised of recombinant human BMP-2, Beta-TCP powder, and a biodegradable polymer: an experimental study in dogs. *J Orthop Res.* 2007;25:1042–1051.
13. Hsu WK, Wang JC. The use of bone morphogenetic protein in spine fusion. *Spine J.* 2008;8:419–425.
14. Itoh H, Ebara S, Kamimura M, Tateiwa Y, Kinoshita T, Yuzawa Y, Takaoka K. Experimental spinal fusion with use of recombinant human bone morphogenetic protein 2. *Spine.* 1999;24:1402–1405.
15. Johnsson R, Stromqvist B, Aspenberg P. Randomized radiostereometric study comparing osteogenic protein-1 (BMP-7) and autograft bone in human noninstrumented posterolateral lumbar fusion: 2002 Volvo Award in clinical studies. *Spine.* 2002;27:2654–2661.
16. Joseph V, Rampersaud YR. Heterotopic bone formation with the use of rhBMP2 in posterior minimal access interbody fusion: a CT analysis. *Spine.* 2007;32:2885–2890.
17. Konishi S, Nakamura H, Seki M, Nagayama R, Yamano Y. Hydroxyapatite granule graft combined with recombinant human bone morphogenic protein-2 for solid lumbar fusion. *J Spinal Disord Tech.* 2002;15:237–244.
18. Kubler NR, Reuther JF, Faller G, Kirchner T, Ruppert R, Sebald W. Inductive properties of recombinant human BMP-2 produced in a bacterial expression system. *Int J Oral Maxillofac Surg.* 1998;27:305–309.
19. Kurz LT, Garfin SR, Booth RE, Jr. Harvesting autogenous iliac bone grafts. A review of complications and techniques. *Spine.* 1989;14:1324–1331.
20. Lewandrowski KU, Nanson C, Calderon R. Vertebral osteolysis after posterior interbody lumbar fusion with recombinant human bone morphogenetic protein 2: a report of five cases. *Spine J.* 2007;7:609–614.
21. Martin GJ, Jr., Boden SD, Marone MA, Marone MA, Moskovitz PA. Posterolateral intertransverse process spinal arthrodesis with rhBMP-2 in a nonhuman primate: important lessons learned regarding dose, carrier, and safety. *J Spinal Disord.* 1999;12:179–186.
22. Minamide A, Kawakami M, Hashizume H, Sakata R, Tamaki T. Evaluation of carriers of bone morphogenetic protein for spinal fusion. *Spine.* 2001;26:933–939.
23. Minamide A, Kawakami M, Hashizume H, Sakata R, Yoshida M, Tamaki T. Experimental study of carriers of bone morphogenetic protein used for spinal fusion. *J Orthop Sci.* 2004;9:142–151.
24. Nakagawa K, Imai Y, Ohta Y, Takaoka K. Prostaglandin E2 EP4 agonist (ONO-4819) accelerates BMP-induced osteoblastic differentiation. *Bone.* 2007;41:543–548.
25. Namikawa T, Terai H, Hoshino M, Kato M, Toyoda H, Yano K, Nakamura H, Takaoka K. Enhancing effects of a prostaglandin EP4 receptor agonist on recombinant human bone morphogenetic protein-2 mediated spine fusion in a rabbit model. *Spine.* 2007;32:2294–2299.
26. Namikawa T, Terai H, Suzuki E, Hoshino M, Toyoda H, Nakamura H, Miyamoto S, Takahashi N, Ninomiya T, Takaoka K. Experimental spinal fusion with recombinant human bone morphogenetic protein-2 delivered by a synthetic polymer and beta-tricalcium phosphate in a rabbit model. *Spine.* 2005;30:1717–1722.
27. Ohta Y, Nakagawa K, Imai Y, Katagiri T, Koike T, Takaoka K. Cyclic AMP enhances Smad-mediated BMP signaling through PKA-CREB pathway. *J Bone Miner Metab.* 2008;26:478–484.
28. Raisz LG. Pathogenesis of osteoporosis: concepts, conflicts, and prospects. *J Clin Invest.* 2005;115:3318–3325.
29. Ruppert R, Hoffmann E, Sebald W. Human bone morphogenetic protein 2 contains a heparin-binding site which modifies its biological activity. *Eur J Biochem.* 1996;237:295–302.
30. Saito N, Okada T, Horiuchi H, Murakami N, Takahashi J, Nawata M, Ota H, Nozaki K, Takaoka K. A biodegradable polymer as a cytokine delivery system for inducing bone formation. *Nat Biotechnol.* 2001;19:332–335.
31. Sandhu HS, Kanim LE, Kabo JM, Toth JM, Zeegen EN, Liu D, Delamarter RB, Dawson EG. Effective doses of recombinant human bone morphogenetic protein-2 in experimental spinal fusion. *Spine.* 1996;21:2115–2122.
32. Santoni BG, Pluhar GE, Motta T, Wheeler DL. Hollow calcium phosphate microcarriers for bone regeneration: in vitro osteoproduction and ex vivo mechanical assessment. *Biomed Mater Eng.* 2007;17:277–289.
33. Sasaoka R, Terai H, Toyoda H, Imai Y, Sugama R, Takaoka K. A prostanoid receptor EP4 agonist enhances ectopic bone formation induced by recombinant human bone morphogenetic protein-2. *Biochem Biophys Res Commun.* 2004;318:704–709.
34. Schimandle JH, Boden SD, Hutton WC. Experimental spinal fusion with recombinant human bone morphogenetic protein-2. *Spine.* 1995;20:1326–1337.
35. Seeherman HJ, Bouxsein M, Kim H, Li R, Li XJ, Aiolova M, Wozney JM. Recombinant human bone morphogenetic protein-2 delivered in an injectable calcium phosphate paste accelerates osteotomy-site healing in a nonhuman primate model. *J Bone Joint Surg Am.* 2004;86:1961–1972.
36. Taguchi S, Namikawa T, Ieguchi M, Takaoka K. Reconstruction of bone defects using rhBMP-2-coated devitalized bone. *Clin Orthop Relat Res.* 2007;461:162–169.
37. Takayanagi H. Osteoimmunology: shared mechanisms and crosstalk between the immune and bone systems. *Nat Rev Immunol.* 2007;7:292–304.
38. Toyoda H, Terai H, Sasaoka R, Oda K, Takaoka K. Augmentation of bone morphogenetic protein-induced bone mass by local delivery of a prostaglandin E EP4 receptor agonist. *Bone.* 2005;37:555–562.
39. Urist MR. Bone: formation by autoinduction. *Science.* 1965;150:893–899.
40. Weigel U, Meyer M, Sebald W. Mutant proteins of human interleukin 2. Renaturation yield, proliferative activity and receptor binding. *Eur J Biochem.* 1989;180:295–300.
41. Wong DA, Kumar A, Jatana S, Ghiselli G, Wong K. Neurologic impairment from ectopic bone in the lumbar canal: a potential complication of off-label PLIF/TLIF use of bone morphogenetic protein-2 (BMP-2). *Spine J.* 2007;8:1011–1018.
42. Wozney JM, Rosen V, Celeste AJ, Mitsock LM, Whitters MJ, Kriz RW, Hewick RM, Wang EA. Novel regulators of bone formation: molecular clones and activities. *Science.* 1988;242:1528–1534.
43. Wu CH, Hara K, Ozawa H. Enhanced osteoinduction by intramuscular grafting of BMP-beta-TCP compound pellets into murine models. *Arch Histol Cytol.* 1992;55:97–112.
44. Yamamoto Y, Udagawa N, Matsuura S, Nakamichi Y, Horiuchi H, Hosoya A, Nakamura M, Ozawa H, Takaoka K, Penninger JM, Noguchi T, Takahashi N. Osteoblasts provide a suitable microenvironment for the action of receptor activator of nuclear factor-kappaB ligand. *Endocrinology.* 2006;147:3366–3374.
45. Yano K, Hoshino M, Ohta Y, Manaka T, Naka Y, Imai Y, Sebald W, Takaoka K. Osteoinductive capacity and heat stability of recombinant human bone morphogenetic protein-2 produced by Escherichia coli and dimerized by biochemical processing. *J Bone Miner Metab.* 2009;27:355–363.
46. Zaidi M. Skeletal remodeling in health and disease. *Nat Med.* 2007;13:791–801.

Eur Spine J (2009) 18:1279–1286
DOI 10.1007/s00586-009-1041-6

ORIGINAL ARTICLE

Factors affecting neurological deficits and intractable back pain in patients with insufficient bone union following osteoporotic vertebral fracture

Masatoshi Hoshino · Hiroaki Nakamura · Hidetomi Terai · Tadao Tsujio · Masaharu Nabeta · Takashi Namikawa · Akira Matsumura · Akinobu Suzuki · Kazushi Takayama · Kunio Takaoka

Received: 18 October 2008 / Revised: 17 March 2009 / Accepted: 12 May 2009 / Published online: 31 May 2009

Abstract The purpose of this study was to examine factors affecting the severity of neurological deficits and intractable back pain in patients with insufficient bone union following osteoporotic vertebral fracture (OVF). Reports of insufficient union following OVF have recently increased. Patients with this lesion have various degrees of neurological deficits and back pain. However, the factors contributing to the severity of these are still unknown. A total of 45 patients with insufficient union following OVF were included in this study. Insufficient union was diagnosed based on the findings of vertebral cleft on plain radiography or CT, as well as fluid collection indicating high-intensity change on T2-weighted MRI. Multivariate logistic regression analysis was performed to determine the factors contributing to the severity of neurological deficits and back pain in the patients. Age, sex, level of fracture, duration after onset of symptoms, degree of local kyphosis, degree of angular instability, ratio of occupation by bony fragments, presence or absence of protrusion of flavum, and presence or absence of ossification of the anterior longitudinal ligament (OALL) in the adjacent level were used as explanatory variables, while severity of neurological deficits and back pain were response variables. On multivariate analysis, factors significantly affecting the severity of neurological deficits were angular instability of more than 15° [adjusted odds ratio (OR), 9.24 (95% confidence interval, CI 1.49–57.2); $P < 0.05$] and ratio of occupation by bony fragments in the spinal canal of more than 42% [adjusted OR 9.23 (95%CI 1.15–74.1); $P < 0.05$]. The factor significantly affecting the severity of back pain was angular instability of more than 15° [adjusted OR 14.9 (95%CI 2.11–105); $P < 0.01$]. On the other hand, presence of OALL in the adjacent level reduced degree of back pain [adjusted OR 0.14 (95%CI 0.03–0.76); $P < 0.05$]. In this study, pronounced angular instability and marked posterior protrusion of bony fragments in the canal were factors affecting neurological deficits. In addition, marked angular instability was a factor affecting back pain. These findings are useful in determining treatment options for patients with insufficient union following OVF.

Keywords Osteoporotic vertebral fracture · Risk factor · Insufficient bone union · Neurological deficit · Back pain

M. Hoshino · H. Nakamura (✉) · H. Terai · T. Tsujio · T. Namikawa · A. Matsumura · A. Suzuki · K. Takayama · K. Takaoka
Department of Orthopedic Surgery, Osaka City University Graduate School of Medicine, 1-4-3 Asahi-machi Abeno-ku, Osaka 545-8585, Japan
e-mail: hnakamura@med.osaka-cu.ac.jp

M. Nabeta
Department of Orthopedic Surgery, Ishikiriseiki Hospital, Osaka, Japan

Introduction

Fracture associated with osteoporosis has become a major problem because the population of elderly individuals has been increasing [4]. Modalities efficacious in preventing as well as treating osteoporosis-associated fractures are thus desired in the coming decade [7]. Among such fractures, vertebral fractures are the most common type with significant morbidity [24].

The osteoporotic vertebral fracture (OVF) has severe impact on activities of daily living and quality of life in

elderly patients and is the beginning of a long-lasting deterioration of the patient's health [28]. Some patients present with intractable back pain for prolonged periods of time, while others suffer from neurological deficits within a few months' time after fracture. In such cases, insufficient union is often noted on plain radiography and/or MRI [18, 22]. Recently, reports of insufficient union have been increasing [13, 15, 19, 26, 29].

Patients with insufficient union following OVF have been treated with various methods conservatively and surgically. Surgical procedures include resection of fractured vertebral bodies and grafting of autologous bone with implants through the anterior approach are one option, while closed-wedge osteotomy through the posterior approach has been another [9, 20, 25, 27]. However, considering the age and comorbidities of affected patients, each of these procedures is rather invasive. Vertebroplasty is less invasive and has been reported to yield successful clinical results for painful OVF, but not to yield satisfactory results for patients with neurological deficits [2, 8, 14, 23].

Thus, the treatment options for insufficient union following OVF have not been clearly established. To elucidate useful treatment options for this lesion, it is necessary to evaluate the factors contributing to neurological deficits and/or intractable back pain associated with this type of fracture. The purpose of this study was to elucidate the factors affecting the severity of neurological deficits and intractable back pain in patients with insufficient bone union following OVF.

Material and methods

Patient population

A total of 45 patients treated for insufficient union following OVF were retrospectively reviewed. Insufficient union was diagnosed based on intravertebral vacuum cleft on plain radiography or CT, as well as fluid collection on T2-weighted MRI within the vertebral body. All patients had continued to complain of symptoms for longer than 2 months (range 2–36 months, mean 6.9 months).

There were 10 men and 35 women whose mean age at the time of diagnosis was 74 years (range 56–87 years). The fracture levels were T9 in 1 patient, T11 in 3, T12 in 22, L1 in 11, L2 in 6, L4 in 1, and L5 in 1. In these patients, bone mineral density was measured in the lumbar spine or femoral neck, and the diagnosis of osteoporosis was confirmed. Other metabolic bone diseases and malignancies such as myeloma and metastatic cancer were excluded. The precipitating events leading to the fracture were fall in 22 patients (48.8%), lift of a heavy object in 5 (11.1%), and no recollection of trauma in 18 (40%). The comorbidities were diabetes in 12 patients (26.7%) and rheumatoid arthritis in four (8.9%) take steroids. For neurological findings, 10 patients had a hyperreflexia and 19 a hyporeflexia in their legs. Twenty-five patients had a sensory deficit. Eleven patients had a sphincter dysfunction.

Eight patients were managed with posterior decompression and fusion surgery, 23 vertebroplasty, and 14 conservative therapies such as a corset or analgesics.

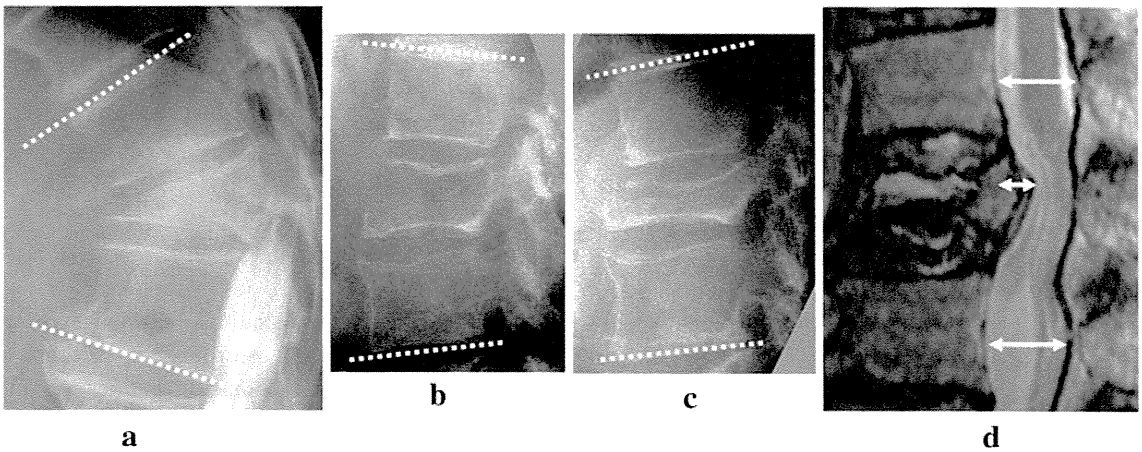

Fig. 1 Radiological assessment. **a** Local kyphosis was calculated as Cobb angle between the upper endplate of the vertebra just cranial to the fractured vertebra and the inferior endplate of the vertebra just caudal to the fractured vertebra on lateral plain X-ray films. **b**, **c** Angular instability was calculated as change in Cobb angle on lateral dynamic radiography (**b** extension, **c** flexion). **d** Ratio of occupation by bony fragments of the spinal canal was calculated as ratio in percentage of bony fragment diameter to adjacent normal canal diameter on mid-sagittal MR images

Table 1 Patient demographics

Characteristics	No. of subjects	Mean or percent
Mean age (years)		74.0
Mean duration of fracture (months)		6.9
Sex		
Male	10	22.2%
Female	35	77.8%
Level of injury		
L2 or below	8	17.8%
L1	11	24.4%
T12 or above	26	57.8%
Mean local kyphosis (°)		24.8
Mean angular instability (°)		11.4
Mean ratio of occupation by bony fragments (%)		38.1
Protrusion of flavum		
Absent	36	80%
Present	9	20%
Adjacent OALL		
Absent	31	71.1%
Present	13	28.9%
Neurological deficits		
None	24	53.3%
Mild	10	22.2%
Severe	11	24.5%
Back pain		
None or mild	7	15.6%
Moderate	16	35.6%
Severe	22	48.8%

Radiological assessment

Local kyphosis was calculated as the Cobb angle between the cranial endplate of the vertebra just cranial to the fracture and the caudal endplate of the vertebra just caudal to the fractured vertebra on lateral plain X-ray films (Fig. 1). Angular instability was calculated as change in vertebral wedge angle on lateral dynamic radiography. Ratio of occupation by bony fragments of the spinal canal was calculated as the ratio in percentage of sagittal diameter of bony fragments to sagittal diameter of the spinal canal on mid-sagittal MR images.

Statistical analysis

As response variables, severities of neurological deficits and of back pain were each graded using three levels. For neurological deficits, "none" was defined as no neurological deficit, "mild" as Manual Muscle Test (MMT) score of grade 4, and "severe" as MMT score of grade 3 or less. For back pain, "none or mild" was defined as VAS score less than 30, "moderate" as VAS score from 30 to 70, and "severe" as VAS score above 70.

Explanatory variables included age, sex, level of fracture, duration of symptoms after onset, angle of local kyphosis, degree of angular instability, ratio of occupation by bony fragments of the spinal canal, presence or absence of protrusion of flavum in the spinal canal, and presence or absence of ossification of the anterior longitudinal ligament (OALL) in the adjacent level. Continuous variables (angle of local kyphosis, degree of angular instability, and ratio of occupation by bony fragments of the spinal canal) were categorized by approximate tertile, except for age, and duration of fracture. Levels of fracture were divided into three categories. The first category was the level cranial to T12, that of the spinal cord. The second category was the level of L1, that of the conus medullaris. The third category was L2 and caudal to L2, the levels of the cauda equina. Other characteristics were treated as dichotomous variables (male/female for sex, present/absent for protrusion of flavum, or adjacent OALL).

To express the associations between severe neurological deficits or severe back pain and explanatory variables, odds ratio (ORs) and their 95% confidence intervals (CIs) were computed using the proportional odds model in logistic regression. We calculated P values for the scores to test the proportional odds assumption in order to confirm that use of the proportional odds model would be appropriate for these models.

All analyses were performed using Statistical Analysis System Version 9.1 (SAS Institute, Inc., Cary, NC, USA). Findings of $P < 0.05$ were considered significant.

Results

Patient demographic variables are shown in Table 1. Overall, 46.7% of patients exhibited mild or severe neurological deficits, with findings of less than grade 4 on MMT, and 84.4% had moderate or severe back pain, with a VAS score of more than 30.

Neurological deficits

Table 2 shows the associations between explanatory variables and severity of neurological deficits. Univariate analysis showed that pronounced angular instability within the affected vertebral body of more than 15° significantly increased the OR of neurological deficits [crude OR, 10.0 (95%CI 2.12–47.7); $P < 0.01$]. Marked spinal canal encroachment by protruding bony fragments was also a factor significantly contributing to neurological deficits. ORs were 6.74 (95%CI 1.11–40.9, $P < 0.05$) for moderate protrusion from 33 to 41% and 11.9 [(95%CI 2.11–68.0);

Table 2 Univariate and multivariate ORs for severity of neurological deficits

Characteristics	Neurological deficits			Univariate		Multivariate	
	None *n*	Mild *n*	Severe *n*	OR (95%CI)	*P* value	OR (95%CI)	*P* value
Age (year) per 1 year				0.96 (0.89–1.04)	0.341	0.91 (0.82–1.02)	0.106
Sex							
Male	5	4	1	1		1	
Female	19	6	10	1.20 (0.31–4.66)	0.794	0.66 (0.12–3.69)	0.634
Level of injury							
L2 or below	4	4	0	1		1	
L1	6	2	3	2.09 (0.37–11.8)	0.406	3.31 (0.31–35.6)	0.323
T12 or above	14	4	8	2.06 (0.47–9.05)	0.341	4.87 (0.66–35.9)	0.120
Duration of fracture (month) per 1 month				0.96 (0.85–1.08)	0.532	0.99 (0.84–1.18)	0.932
Local kyphosis (°)							
−21	5	6	2	1		1	
22–28	10	3	2	0.45 (0.10–1.94)	0.281	0.31 (0.04–2.44)	0.263
29+	9	1	7	1.14 (0.29–4.37)	0.855	0.62 (0.08–4.97)	0.653
Angular instability(°)							
−7	12	1	2	1		1	
8–14	7	5	1	2.59 (0.51–13.2)	0.252	2.20 (0.25–19.6)	0.479
15+	5	4	8	10.0 (2.12–47.7)	0.004	9.24 (1.49–57.2)	0.017
Ratio of occupation by bony fragments (%)							
−32	12	1	1	1		1	
33–41	5	6	2	6.74 (1.11–40.9)	0.038	2.35 (0.29–18.9)	0.421
42+	7	3	8	11.9 (2.11–68.0)	0.005	9.23 (1.15–74.1)	0.037
Protrusion of flavum							
Absent	21	7	8	1		1	
Present	3	3	3	2.27 (0.58–8.94)	0.241	0.56 (0.08–4.06)	0.569
Adjacent OALL							
Absent	17	8	7	1		1	
Present	7	2	4	1.15 (0.34–3.89)	0.828	1.79 (0.35–9.26)	0.483

OR odds ratio, *CI* confidence interval

$P < 0.01$] for severe protrusion of more than 42%. No other explanatory variables examined significantly contributed to neurological deficits on univariate analysis.

Multivariate analysis showed that pronounced angular instability in the upper tertile, of more than 15°, and high ratio of occupation by bony fragments, in the upper tertile of more than 42%, were factors significantly contributing to the degree of neurological deficit [adjusted OR 9.24 (95%CI 1.49–57.2); $P < 0.05$ and adjusted OR 9.23 (95%CI 1.15–74.1); $P < 0.05$, respectively]. No other variables examined were significant factors on multivariate analysis (Fig. 2).

Intractable back pain

Table 3 shows the associations between explanatory variables and severity of back pain in patients with insufficient union following OVF. Univariate analysis revealed that moderate angular instability ranging from 8° to 14° had an OR of 4.45 [(95%CI 1.01–19.6); $P < 0.05$)] while marked angular instability of more than 15° had an OR of 9.83 [(95%CI 2.19–44.1); $P < 0.01$). No other variables examined were significant factors on univariate analysis.

Multivariate analysis showed that pronounced angular instability of more than 15° was a factor significantly contributing to intractable pain [adjusted OR 14.9 (95%CI 2.11–105); $P < 0.01$]. On the other hand, the existence of OALL in the level adjacent to the fracture was a factor reducing the degree of back pain [adjusted OR 0.14 (95%CI 0.03–0.76); $P < 0.05$]. No other variables examined were significant factors on multivariate analysis.

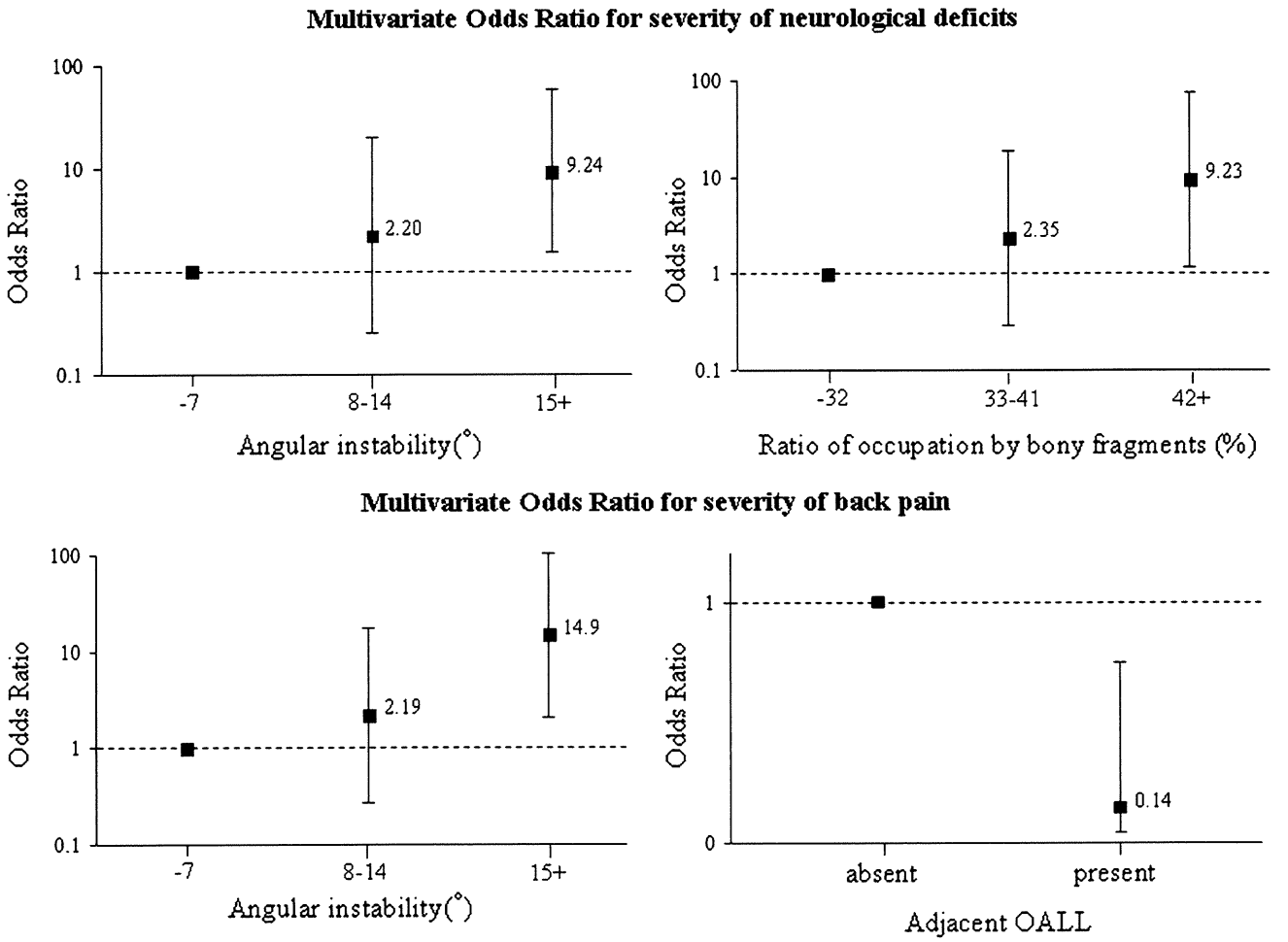

Fig. 2 Multivariate odds ratios for severity of neurological deficits and back pain. The *y* axis is on a log scale. The *I bars* denote 95% confidence intervals

Discussion

The pain associated with OVF usually improves if there is no severe residual deformity. Ettinger et al. reported that vertebral deformities cause marked back pain if vertebral height ratios fall four standard deviations below the normal mean [6]. However, pseudoarthrosis following OVF has recently come to be considered a poor prognostic factor for prolonged and intractable pain [10, 14, 16]. On the other hand, Hashidate et al. reported that in 66.7% of patients back pain decreased naturally despite the presence of vertebral instability in cases of vertebral pseudoarthrosis [11]. Thus, not all patients with non-union exhibited prolonged and intractable back pain. As noted above, the factors causing prolonged and intractable back pain in the case of insufficient bone union following OVF are still unknown. Toyone et al. reported a significant correlation between back pain and changes in wedging rate from supine to standing positions for OVF of recent onset [31]. In the present study, marked angular instability of the affected vertebral body significantly contributed to severity of back pain.

The presence of an intravertebral cleft had been reported to be a risk factor for progressive vertebral collapse inducing neurological deficits [15, 17]. A few previous studies investigated the relationship between neurological deficits and radiological findings. Hashimoto et al. reported that ratios of occupation by bone fragments in the spinal canal of more than 35% at epiconus level, more than 45% at conus medullaris level, and more than 55% at cauda equina level were factors significantly associated with neurological impairment in traumatic burst fracture [12]. Trafton et al. reported that burst fracture at T12 or L1 with canal encroachment of more than 50% of mid-sagittal canal diameter was a significant risk factor for neurological impairment [32]. These reports were both on acute traumatic vertebral fracture. Nguyen et al. reported a series of ten patients with osteoporotic vertebral burst fracture, which led to varying degrees of neurologic compromise. In their cases, mean

Table 3 Univariate and multivariate ORs for severity of back pain

Characteristics	Back pain			Univariate		Multivariate	
	None or mild *n*	Moderate *n*	Severe *n*	OR (95%CI)	*P* value	OR (95%CI)	*P* value
Age (year) per 1 year				0.98 (0.91–1.06)	0.658	1.05 (0.94–1.18)	0.406
Sex							
Male	2	4	4	1		1	
Female	5	12	18	1.56 (0.42–5.84)	0.509	2.15 (0.43–10.6)	0.348
Level of injury							
L2 or below	0	2	6	1		1	
L1	1	7	3	0.24 (0.04–1.48)	0.125	0.15 (0.01–213)	0.160
T12 or above	6	7	13	0.30 (0.06–1.44)	0.133	0.20 (0.02–1.96)	0.165
Duration of fracture (month) per 1 month				0.96 (0.87–1.07)	0.459	0.97 (0.83–1.14)	0.715
Local kyphosis (°)							
−21	1	3	9	1		1	
22–28	3	5	7	0.36 (0.08–1.63)	0.186	0.72 (0.10–5.35)	0.751
29+	3	8	6	0.28 (0.06–1.20)	0.086	0.37 (0.04–3.36)	0.377
Angular instability(°)							
−7	6	5	4	1		1	
8–14	0	7	6	4.45 (1.01–19.6)	0.048	2.19 (0.28–17.2)	0.456
15+	1	4	12	9.83 (2.19–44.1)	0.003	14.9 (2.11–105)	0.007
Ratio of occupation by bony fragments (%)							
−32	3	5	6	1		1	
33–41	1	3	9	3.19 (0.69–14.7)	0.137	4.72 (0.65–34.2)	0.124
42+	3	8	7	0.99 (0.27–3.63)	0.983	0.47 (0.07–3.29)	0.445
Protrusion of flavum							
Absent	5	13	18	1		1	
Present	2	3	4	0.72 (0.18–2.84)	0.958	4.04 (0.47–34.6)	0.202
Adjacent OALL							
Absent	3	11	18	1		1	
Present	4	5	4	0.30 (0.09–1.05)	0.059	0.14 (0.03–0.76)	0.023

OR odds ratio, *CI* confidence interval

canal compromise was 41% [21]. No reports were found in our review of the literature on the relationship between neurological deficits and intravertebral instability. Baba et al. reported 27 patients who suffered osteoporotic vertebral collapse with late neurological complications. They considered the pathology in this lesion to involve abnormal hypermobility at the fractured spinal level with gradual retropulsion of fractured fragments into the spinal canal, resulting in late paralysis [1].

In the present study, it was found that intravertebral instability contributes to the degree of neurological deficits in cases of insufficient union following OVF. Stabilization of the lesion site without decompression is, thus, a treatment option for this condition. Some studies have reported that treatment with immobilization without decompression, such as conservative management using a plaster body cast, vertebroplasty, or posterior in situ stabilization, could result in neurological improvement with progression of bone union [3, 5, 30]. These findings suggest that spinal instability is related to the pathogenesis of neurological deficits.

In this study, the factors significantly contributing to neurological deficits were angular instability of more than 15° and ratio of occupation by bony fragments of the spinal canal of more than 42%. The factors contributing to severity of back pain were angular instability of more than 15° and absence of OALL in the adjacent segment. As noted above, intravertebral angular instability was a factor common to neurological deficits and back pain. Stabilization of the fractured vertebra thus appears to be the most important treatment option for insufficient fracture following OVF. In patients with bony encroachment of higher percentage, decompression is needed to obtain satisfactory surgical results.

Conclusions

In conclusion, we investigated the factors contributing to the severity of symptoms in patients with insufficient union following OVF. Factors significantly contributing to the severity of neurological deficits were angular instability of more than 15° within the affected vertebral body and ratio of occupation by bony fragments in the spinal canal of more than 42%. Factors significantly contributing to the severity of back pain were angular instability of more than 15° and absence of adjacent OALL. Angular instability was thus a factor common to both neurological deficits and prolonged back pain.

References

1. Baba H, Maezawa Y, Kamitani K, Furusawa N, Imura S, Tomita K (1995) Osteoporotic vertebral collapse with late neurological complications. Paraplegia 33:281–289
2. Barr JD, Barr MS, Lemley TJ, McCann RM (2000) Percutaneous vertebroplasty for pain relief and spinal stabilization. Spine 25:923–928. doi:10.1097/00007632-200004150-00005
3. Braakman R, Fontijne WP, Zeegers R, Steenbeek JR, Tanghe HL (1991) Neurological deficit in injuries of the thoracic and lumbar spine. A consecutive series of 70 patients. Acta Neurochir (Wien) 111:11–17. doi:10.1007/BF01402507
4. Cummings SR, Melton LJ (2002) Epidemiology and outcomes of osteoporotic fractures. Lancet 359:1761–1767. doi:10.1016/S0140-6736(02)08657-9
5. de Klerk LW, Fontijne WP, Stijnen T, Braakman R, Tanghe HL, van Linge B (1998) Spontaneous remodeling of the spinal canal after conservative management of thoracolumbar burst fractures. Spine 23:1057–1060. doi:10.1097/00007632-199805010-00018
6. Ettinger B, Black DM, Nevitt MC, Rundle AC, Cauley JA, Cummings SR, Genant HK (1992) Contribution of vertebral deformities to chronic back pain and disability. The Study of Osteoporotic Fractures Research Group. J Bone Miner Res 7:449–456
7. Fujiwara S (2005) Epidemiology of osteoporosis in Japan. J Bone Miner Metab 23(Suppl):81–83. doi:10.1007/BF03026329
8. Garfin SR, Yuan HA, Reiley MA (2001) New technologies in spine: kyphoplasty and vertebroplasty for the treatment of painful osteoporotic compression fractures. Spine 26:1511–1515. doi:10.1097/00007632-200107150-00002
9. Gertzbein SD, Harris MB (1992) Wedge osteotomy for the correction of post-traumatic kyphosis. A new technique and a report of three cases. Spine 17:374–379. doi:10.1097/00007632-199203000-00025
10. Hasegawa K, Homma T, Uchiyama S, Takahashi H (1998) Vertebral pseudarthrosis in the osteoporotic spine. Spine 23:2201–2206. doi:10.1097/00007632-199810150-00011
11. Hashidate H, Kamimura M, Nakagawa H, Takahara K, Uchiyama S (2006) Pseudoarthrosis of vertebral fracture:radiographic and characteristic clinical fractures and natural history. J Orthop Sci 11:28–33. doi:10.1007/s00776-005-0967-8
12. Hashimoto T, Kaneda K, Abumi K (1988) Relationship between traumatic spinal canal stenosis and neurologic deficits in thoracolumbar burst fractures. Spine 13:1268–1272. doi:10.1097/00007632-198811000-00011
13. Heggeness MH (1993) Spine fracture with neurological deficit in osteoporosis. Osteoporos Int 3:215–221. doi:10.1007/BF01623679
14. Hoshino M, Nakamura H, Konishi S, Nagayama R, Terai H, Tsujio T, Namikawa T, Kato M, Takaoka K (2006) Endoscopic vertebroplasty for the treatment of chronic vertebral compression fracture. Technical note. J Neurosurg Spine 5:461–467. doi:10.3171/spi.2006.5.5.461
15. Ito Y, Hasegawa Y, Toda K, Nakahara S (2002) Pathogenesis and diagnosis of delayed vertebral collapse resulting from osteoporotic spinal fracture. Spine J 2:101–106. doi:10.1016/S1529-9430(01)00165-6
16. Jang JS, Kim DY, Lee SH (2003) Efficacy of percutaneous vertebroplasty in the treatment of intravertebral pseudarthrosis associated with noninfected avascular necrosis of the vertebral body. Spine 28:1588–1592. doi:10.1097/00007632-200307150-00021
17. Kaneda K, Asano S, Hashimoto T, Satoh S, Fujiya M (1992) The treatment of osteoporotic posttraumatic vertebral collapse using the Kaneda device and bioactive ceramic vertebral prosthesis. Spine 17:S295–S303. doi:10.1097/00007632-199208001-00015
18. Kim DY, Lee SH, Jang JS, Chung SK, Lee HY (2004) Intravertebral vacuum phenomenon in osteoporotic compression fracture: report of 67 cases with quantitative evaluation of intravertebral instability. J Neurosurg 100:24–31
19. Lafforgue P, Chagnaud C, Daumen-Legre V, Daver L, Kasbarian M, Acquaviva PC (1997) The intravertebral vacuum phenomenon ("vertebral osteonecrosis"). Migration of intradiscal gas in a fractured vertebral body? Spine 22:1885–1891. doi:10.1097/00007632-199708150-00015
20. Mochida J, Toh E, Chiba M, Nishimura K (2001) Treatment of osteoporotic late collapse of a vertebral body of thoracic and lumbar spine. J Spinal Disord 14:393–398. doi:10.1097/00002517-200110000-00004
21. Nguyen HV, Ludwig S, Gelb D (2003) Osteoporotic vertebral burst fractures with neurologic compromise. J Spinal Disord Tech 16:10–19
22. Peh WC, Gelbart MS, Gilula LA, Peck DD (2003) Percutaneous vertebroplasty: treatment of painful vertebral compression fractures with intraosseous vacuum phenomena. AJR Am J Roentgenol 180:1411–1417
23. Phillips FM (2003) Minimally invasive treatments of osteoporotic vertebral compression fractures. Spine 28:S45–S53. doi:10.1097/00007632-200308011-00009
24. Ross PD, Fujiwara S, Huang C, Davis JW, Epstein RS, Wasnich RD, Kodama K, Melton LJIII (1995) Vertebral fracture prevalence in women in Hiroshima compared to Caucasians or Japanese in the US. Int J Epidemiol 24:1171–1177. doi:10.1093/ije/24.6.1171
25. Saita K, Hoshino Y, Kikkawa I, Nakamura H (2000) Posterior spinal shortening for paraplegia after vertebral collapse caused by osteoporosis. Spine 25:2832–2835. doi:10.1097/00007632-200011010-00018
26. Sarli M, Perez Manghi FC, Gallo R, Zanchetta JR (2005) The vacuum cleft sign: an uncommon radiological sign. Osteoporos Int 16:1210–1214. doi:10.1007/s00198-005-1833-4
27. Suk SI, Kim JH, Lee SM, Chung ER, Lee JH (2003) Anterior–posterior surgery versus posterior closing wedge osteotomy in posttraumatic kyphosis with neurologic compromised osteoporotic fracture. Spine 28:2170–2175. doi:10.1097/01.BRS.0000090889.45158.5A
28. Suzuki N, Ogikubo O, Hansson T (2008) The course of the acute vertebral body fragility fracture: its effect on pain, disability and quality of life during 12 months. Eur Spine J 17:1380–1390. doi:10.1007/s00586-008-0753-3
29. Theodorou DJ (2001) The intravertebral vacuum cleft sign. Radiology 221:787–788. doi:10.1148/radiol.2213991129

30. Toyone T, Tanaka T, Kato D, Kaneyama R, Otsuka M (2006) The treatment of acute thoracolumbar burst fractures with transpedicular intracorporeal hydroxyapatite grafting following indirect reduction and pedicle screw fixation: a prospective study. Spine 31:E208–E214
31. Toyone T, Tanaka T, Wada Y, Kamikawa K, Ito M, Kimura K, Yamasita T, Matsushita S, Shiboi R, Kato D, Kaneyama R, Otsuka M (2006) Changes in vertebral wedging rate between supine and standing position and its association with back pain: a prospective study in patients with osteoporotic vertebral compression fractures. Spine 31:2963–2966. doi:10.1097/01.brs.0000247802.91724.7e
32. Trafton PG, Boyd CA Jr (1984) Computed tomography of thoracic and lumbar spine injuries. J Trauma 24:506–515. doi:10.1097/00005373-198406000-00008

Repair of Large Osteochondral Defects in Rabbits Using Porous Hydroxyapatite/Collagen (HAp/Col) and Fibroblast Growth Factor-2 (FGF-2)

Hidetsugu Maehara,[1] Shinichi Sotome,[1,2] Toshitaka Yoshii,[1] Ichiro Torigoe,[1] Yuichi Kawasaki,[1] Yumi Sugata,[1,3] Masato Yuasa,[1,3] Masahiro Hirano,[4] Naomi Mochizuki,[4] Masanori Kikuchi,[5] Kenichi Shinomiya,[1,3,6,7] Atsushi Okawa[1]

[1]Department of Orthopaedic and Spinal Surgery, Graduate School, Tokyo Medical and Dental University, 1-5-45 Yushima, Bunkyo-ku, Tokyo 113-8519, Japan, [2]Development Division of Advanced Orthopaedic Therapeutics, Graduate School, Tokyo Medical and Dental University, 1-5-45 Yushima, Bunkyo-ku, Tokyo 113-8519, Japan, [3]Global Center of Excellence (GCOE) Program, International Research Center for Molecular Science in Tooth and Bone Disease, Tokyo Medical and Dental University, 1-5-45 Yushima, Bunkyo-ku, Tokyo 113-8519, Japan, [4]PENTAX New Ceramics Division, HOYA Corporation, 2-36-9 Maeno-cho, Itabashi-ku, Tokyo 174-8639, Japan, [5]Biomaterial Center, National Institute for Materials Science, 1-1 Namiki, Tsukuba, Ibaraki 305-0044, Japan, [6]Hard Tissue Genome Research Center, Tokyo Medical and Dental University, 2-3-10 Kanda-Surugadai, Chiyoda-ku, Tokyo 101-0062, Japan, [7]Core to Core Program for Advanced Bone and Joint Science, Tokyo Medical and Dental University, 2-3-10 Kanda-Surugadai, Chiyoda-ku, Tokyo 101-0062, Japan

Received 20 January 2009; accepted 14 September 2009
Published online in Wiley InterScience (www.interscience.wiley.com). DOI 10.1002/jor.21032

ABSTRACT: Articular cartilage has a limited capacity for self-renewal. This article reports the development of a porous hydroxyapatite/collagen (HAp/Col) scaffold as a bone void filler and a vehicle for drug administration. The scaffold consists of HAp nanocrystals and type I atelocollagen. The purpose of this study was to investigate the efficacy of porous HAp/Col impregnated with FGF-2 to repair large osteochondral defects in a rabbit model. Ninety-six cylindrical osteochondral defects 5 mm in diameter and 5 mm in depth were created in the femoral trochlear groove of the right knee. Animals were assigned to one of four treatment groups: porous HAp/Col impregnated with 50 μl of FGF-2 at a concentration of 10 or 100 μg/ml (FGF10 or FGF100 group); porous HAp/Col with 50 μl of PBS (HAp/Col group); and no implantation (defect group). The defect areas were examined grossly and histologically. Subchondral bone regeneration was quantified 3, 6, 12, and 24 weeks after surgery. Abundant bone formation was observed in the HAp/Col implanted groups as compared to the defect group. The FGF10 group displayed not only the most abundant bone regeneration but also the most satisfactory cartilage regeneration, with cartilage presenting a hyaline-like appearance. These findings suggest that porous HAp/Col with FGF-2 augments the cartilage repair process. © 2009 Orthopaedic Research Society. Published by Wiley Periodicals, Inc. J Orthop Res

Keywords: osteochondral repair; porous hydroxyapatite/collagen; fibroblast growth factor-2; scaffold; tissue engineering

Articular cartilage defects display a poor capacity for repair after injury because the tissue is avascular with a low level of mitotic cellular activity. Thus, damaged lesions in articular cartilage result in progressive deterioration and eventual osteoarthritis.[1] Several factors affect the healing process of these lesions. First, partial thickness defects that do not injure the subchondral bone display minimal healing. In contrast, full-thickness defects that penetrate the subchondral bone receive an abundant source of pluripotent marrow-derived mesenchymal cells for cartilage repair.[2] Second, fibrous or fibrocartilaginous tissues generally fill the defect site, and a limited amount of hyaline cartilage is found.

In recent years, several clinical methods have been used to repair cartilage lesions, including stimulation of the marrow by microfracture, mosaicplasty, and cell-based therapies. However, these methods have not always provided satisfactory results and have presented problems in clinical practice because the regenerated cartilage is morphologically, biochemically, and biomechanically inferior to the original cartilage.[3]

Various growth factors, including fibroblast growth factor-2 (FGF-2),[4] bone morphogenetic protein (BMP),[5–7] transforming growth factor-β (TGF-β)[8] and hepatocyte growth factor (HGF)[9] have also been applied to articular cartilage defects to promote repair. FGF-2 has received considerable attention because of its potential for clinical applications. FGF-2 is known as a chondrocyte mitogen [10] that is found in normal cartilage;[11] it can stimulate chondrocytes to synthesize cartilaginous matrix.[12,13] Although several studies have documented the utility of FGF-2 for cartilage repair,[15,16] disagreements exist regarding the effective doses for large osteochondral defect repair and FGF-2 carrier materials.

In our previous work, we developed a porous hydroxyapatite/collagen (HAp/Col) scaffold consisting of hydroxyapatite nanocrystals and type I atelocollagen.[17,18] The porous HAp/Col has the distinctive characteristics of bioabsorbability, elasticity, and excellent handling, and has been demonstrated to be a suitable material for use as a bone void filler and as a carrier of BMPs.[19–21] We hypothesized that porous HAp/Col with FGF-2 would accelerate subchondral bone repair when used to repair osteochondral defects, and that the local delivery of FGF-2 would promote cartilage repair compared to defects without treatment or defects treated with porous HAp/Col alone.

MATERIALS AND METHODS

Preparation of Porous HAp/Col

HAp/Col nanocomposite fibers were synthesized from atelocollagen derived from porcine skin, $Ca(OH)_2$ and H_3PO_4 using a coprecipitation method, according to a previous report by

Correspondence to: Shinichi Sotome (T: +81-3-5803-5272, F: +81-3-5803-5272; E-mail: sotome.orth@tmd.ac.jp)

Kikuchi et al.[17] In brief, a $Ca(OH)_2$ suspension and a H_3PO_4 solution containing type I atelocollagen (Nitta Gelatin Co., Osaka, Japan) were added to distilled water at 40°C, maintained at a pH of 9.0. The HAp/Col weight ratio was 80:20. The nanocomposite suspension was washed with distilled water and lyophilized.

Lyophilized composites (1 g) were homogenized with 6.5 ml of phosphate-buffered saline (PBS) and alkalized with 50 μl of 1 M sodium hydroxide solution. The solution was mixed with 1.5 ml of 0.6% collagen solution dissolved in phosphoric acid (pH 2.0). The resulting mixture was adjusted to pH 7.0 and infused into a mold. To initiate gelation of the collagen as a binder, the mold containing the mixture was incubated at 37°C for 2 h. The gelated HAp/Col was then frozen at −60°C. Freezing resulted in the growth of ice crystals, which were converted to pores by subsequent lyophilization. The lyophilized porous HAp/Col composite was cross-linked by thermal dehydration at 140°C for 12 h under vacuum and then cut into cylinders 5 mm in diameter and 3 mm in height (Fig. 1B). The porous HAp/Col composites were sterilized by gamma irradiation.

Surgical Procedures

All animal experiments were conducted according to the guidelines provided by the animal committee of the Tokyo Medical and Dental University. Ninety-six skeletally mature male Japanese white rabbits weighing 2.7–3.5 kg were used. The animals were anesthetized by intramuscular administration of medetomidine hydrochloride (0.5 mg/kg) and ketamine hydrochloride (25 mg/kg). Anesthesia was maintained by intramuscular injection at 30-min intervals of half doses of the above solution. The right knee was operated on under sterile conditions. After a medial parapatellar skin incision, the patella was dislocated laterally. One full-thickness cylindrical osteochondral defect, 5 mm in diameter and 5 mm deep, was created in the center of the trochlear groove of the femur using a trephine and a drill-bit with continuous saline irrigation (Fig. 1A). After all debris was removed by flushing with saline, the implants were transplanted. The implants were prepared as follows: Porous HAp/Col was impregnated with 50 μl of recombinant human FGF-2 solution (Kaken Pharmaceutical Co., Ltd., Tokyo, Japan) by pipette at a concentration of 10 or 100 μg/ml and incubated at 4°C for 24 h (FGF10 or FGF100 group); alternatively, porous HAp/Col was impregnated with 50 μl of PBS (HAp/Col group). The doses were determined according to previous reports.[14–16] All implants were placed at the subchondral bone level 2 mm beneath the surface of the adjacent cartilage to permit a good connection between the bone marrow and the cartilage defect (Fig. 1C). Defects without implants comprised the control group (defect group). The joint capsule, the fascial layer, and the skin were closed. After the operation, all rabbits were allowed to move freely in the cages, without any splints. Animals were sacrificed with an overdose of sodium pentobarbital at 3, 6, 12, or 24 weeks after the operation ($n = 6$ in each group).

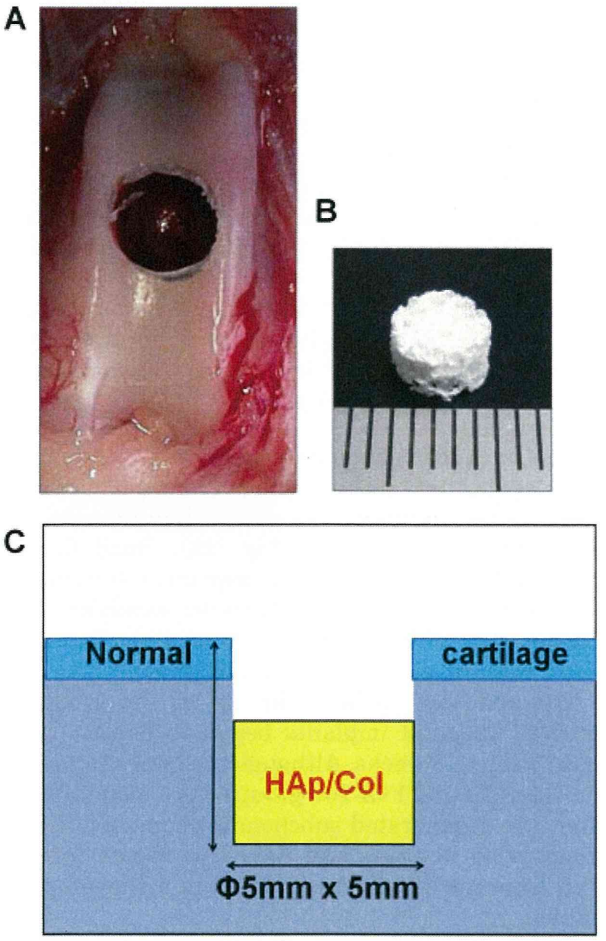

Figure 1. Surgical procedures: (A) Macroscopic observation of an osteochondral defect (5 mm in diameter and 5 mm in depth) in the patellar groove of the right distal femur; (B) cylindrical porous HAp/Col (5 mm in diameter and 3 mm in height) with or without FGF-2 was placed at the subchondral bone level; (C) illustration of the method used for transplantation.

Macroscopic Examination

The harvested knee joints were macroscopically assessed for adhesions, osteoarthritic changes, and synovitis. The appearance of the restored cartilage in terms of color, integrity, and smoothness was also examined. The distal femurs were resected and photographed.

Micro-Computed Tomography Images

To compare the subchondral bone regeneration in each group, the harvested tissues were evaluated with a micro-computed tomography (micro-CT) scanner (ScanXamte-E090, Comscantecno Co. Ltd., Tokyo, Japan). After scanning and reconstruction, each image was displayed in a sagittal view. Regenerated subchondral bone was quantitatively analyzed using bone analysis software (TRI/3D-BON, Ratoc System Engineering Co. Ltd., Tokyo, Japan). The volume of regenerated bone in the defect was quantified as a percentage of the total tissue volume of the defect.

Histological Examination

After fixation with 4% paraformaldehyde solution, the specimens were decalcified in 20% ethylenediaminetetraacetic acid solution and embedded in paraffin. Sections of 5 μm thickness were cut sagittally through the center of the defect site and were stained with either hematoxylin and eosin or with toluidine blue, or else were used for immunohistochemical examination.

Immunohistochemical Examination

Sections were stripped of paraffin using xylene and then dehydrated through graded alcohols. For antigen retrieval, the sections were pretreated with 0.4 mg/ml proteinase K (DAKO, Carpinteria, CA) in Tris-HCl for 15 min at room

temperature. Sections were then treated with 3% H_2O_2 for 15 min to quench endogenous peroxidase activity and incubated in PBS containing 10% normal horse serum at room temperature for 20 min to block nonspecific staining. Sections were then incubated with primary antibodies (mouse anti-human anti-type I and type II collagen; Daiichi Fine Chemical, Toyama, Japan) at room temperature for 1 h. The sections were treated with a secondary biotinylated horse anti-mouse IgG antibody (Vector Laboratories, Burlingame, CA) at room temperature for 30 min and immunostained with VECTASTAIN ABC reagent (Vector Laboratories) and diaminobenzidine. The slides were counterstained with Mayer's hematoxylin.

Histological Scoring

For semiquantitative analysis of the repaired tissue, histological sections were scored blindly by three expert observers according to a modified version of the histological grading scale, as described by Wakitani et al. [22] The scale consists of six categories (cell morphology, matrix staining, surface regularity, thickness of cartilage, regenerated subchondral bone, and integration with adjacent cartilage) scored on a scale from 0 to 16 points, where 16 denotes completely normal tissue (Table 1).

Table 1. Histological Scoring System

Category	Point
Cell morphology	
Hyaline cartilage	4
Mostly hyaline cartilage	3
Mostly fibrocartilage	2
Mostly non-cartilage	1
Non-cartilage only	0
Matrix-staining (metachromasia)	
Normal	3
Slightly reduced	2
Markedly reduced	1
No metachromatic staining	0
Surface regularity[a]	
Smooth	3
Moderate	2
Irregular	1
Severely irregular	0
Thickness of cartilage (%)[b]	
121–150	1
81–120	2
51–80	1
0–50	0
Regenerated subchondral bone	
Good	2
Moderate	1
Poor	0
Integration with adjacent cartilage	
Both edges integrated	2
One edge integrated	1
Neither edge integrated	0
Total maximum	16

[a]Total smooth area of the reparative cartilage compared with the entire area of the cartilage defect.
[b]Average thickness of the reparative cartilage compared with that of the surrounding cartilage.

Statistical Analyses

Histological scoring data and bone volume were analyzed using two-factor ANOVA followed by a multiple comparison test using the Tukey HSD test. Differences were considered statistically significant when the p-value was <0.05.

RESULTS

Macroscopic Observation

No joint contracture, infection, osteoarthritic change, or obvious synovitis was found in any rabbits.

At 3 weeks following injury (Fig. 2A), the regenerated defects in the HAp/Col and FGF10 groups began to fill with whitish opaque tissue from peripheral areas, although the regenerative areas were clearly distinguishable from the normal cartilage. In contrast, the defects in the defect and FGF100 groups remained almost empty, and the bottoms of the defects were covered with reddish granulated tissue.

At 6 weeks (Fig. 2A), larger portions of the defects in the FGF10 group were covered with white regenerated tissue extending from peripheral areas to the central portion. Cartilage regeneration in the FGF100 group was almost equal to that in the HAp/Col group, but was inferior to that in the FGF10 group. The defects in the defect group showed regeneration in the peripheral areas, but the reparative tissue surface was irregular and concave.

At 12 weeks (Fig. 2A), the newly formed tissue in the FGF10 group appeared glossy, smooth, and similar to neighboring normal cartilage. No obvious margins could be distinguished. The defects in the other groups were for the most part filled with whitish rough tissues or were sometimes concave.

At 24 weeks (Fig. 2A), the reparative tissue surface was glistening and smooth (similar to normal cartilage) in the FGF10 group, while it appeared white, opaque, and irregular in the other groups.

Micro-Computed Tomography Images

The regenerated subchondral bone was evaluated using micro-CT images in sagittal planes that passed through the center of the defect (Fig. 2A). Bone formation in the defect group was very poor up to 6 weeks after the operation. Even at 12 or 24 weeks, subchondral bone regeneration in the defect group was incomplete. The defect centers often remained unrepaired.

The subchondral bone defects in the groups that received HAp/Col implants began to exhibit signs of restoration at 3 weeks. Although the bone restoration in the HAp/Col and FGF100 groups were moderate thereafter, the regenerated subchondral bone in the FGF10 group grew in thick and flat. This tissue integrated with adjacent normal bone tissue in a time-dependent fashion.

Quantitative analysis of regenerated subchondral bone (Fig. 2B) showed that, in comparison to the defect group, significantly more subchondral bone was formed in the three groups that were implanted with HAp/Col (Fig. 2C). In particular, the bone volume in the FGF10

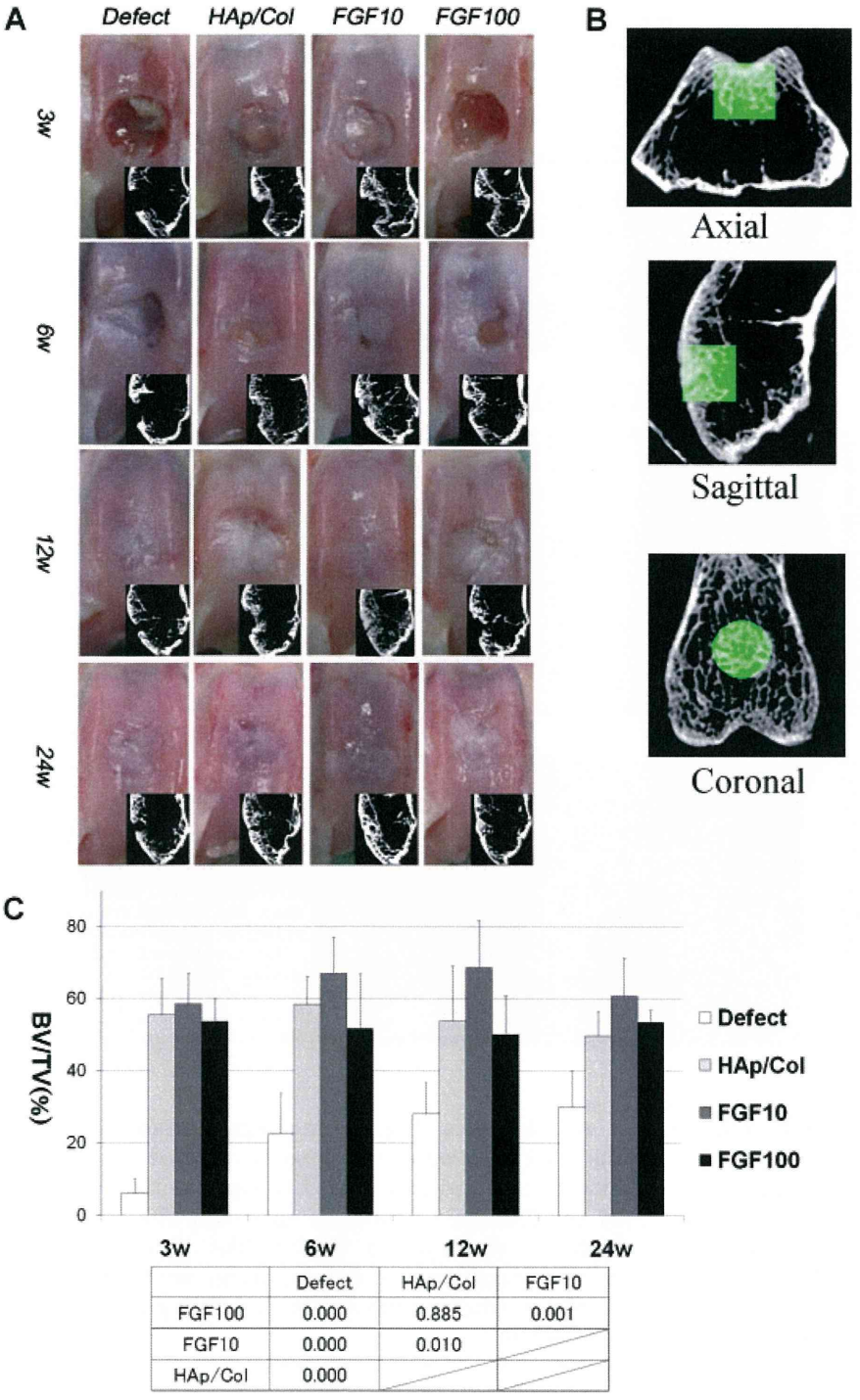

	Defect	HAp/Col	FGF10
FGF100	0.000	0.885	0.001
FGF10	0.000	0.010	
HAp/Col	0.000		

Figure 2. Representative macroscopic observation and micro-CT images of osteochondral defects: (A) Gross appearance and sagittally reconstructed micro-CT images of a representative specimen from each group at 3, 6, 12, and 24 weeks postoperatively; (B) reconstructed micro-CT images that were used to analyze bone volume defects (green areas of each plane); (C) ratios of regenerated bone volume (BV) to the tissue volume (TV) of the defects. The graph indicates mean values and standard deviations; *p*-values of overall data across all time points between each group are shown in the panel under the graph.

group was greater than the volume in the other three groups, and this finding was statistically significant.

Histological Observations

At 3 weeks (Fig. 3), the defects in the defect group were filled with fibrous tissue, no new bone formation was identified, and the cartilaginous extracellular matrix was very poorly developed. Restoration of the defects in animals implanted with HAp/Col with or without FGF-2 was more advanced than that of those in the defect group; notably, most of the implants persisted. The subchondral areas of the defects that were treated with HAp/Col were regenerated with new bone from the periphery of the implant. Superficial layers were also regenerated with cartilage-like tissue from the peripheral areas of the defects. Most importantly, the defects in the FGF10 group were filled with abundant new bone

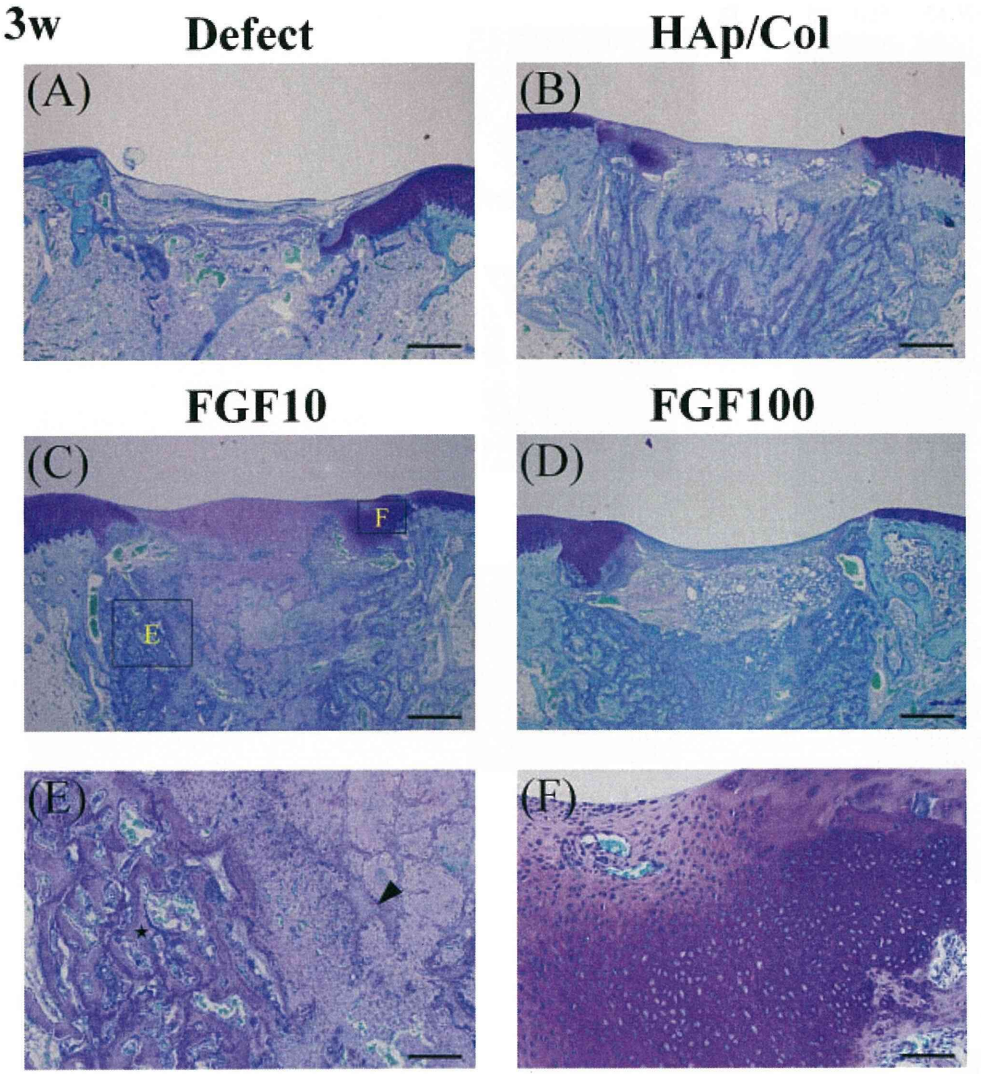

Figure 3. Histological observation at 3 weeks: Sagittal sections stained with toluidine blue taken from the defect group (A), HAp/Col group (B), FGF10 group (C), or FGF100 group (D). Panels (E) and (F) show the framed areas in panel (C) at higher magnification. In panel (E), the arrowhead indicates the remaining HAp/Col and the star indicates the newly formed bone. Scale bars represent 1 mm for (A–D), 300 μm for (E), and 125 μm for (F).

and cartilage matrix from the deep and peripheral areas.

At 6 weeks, the defects in each group improved as compared with those observed at 3 weeks. In comparison with other groups, the defects in the FGF10 group appeared to be satisfactorily regenerated. The tissue from the FGF10 group was primarily composed of round chondrocytes, and the matrix was more distinctly stained with toluidine blue, although fissures or concavities were sometimes observed.

At 12 weeks (Fig. 4), the repaired tissues in the defect, HAp/Col, and FGF100 groups were mainly fibrocartilaginous or fibrous with surface irregularities, and fissures or concave areas were frequently observed. In the FGF10 group, the defects were mostly filled with hyaline-like cartilage with a regular surface that was well-integrated with the native cartilage. An abundance of cartilage matrix could be identified by toluidine blue staining; immunostaining revealed the presence of type II, but not type I collagen. Continuous subchondral bone was well-formed, and the border between regenerated cartilage and subchondral bone was clear.

At 24 weeks (Fig. 5), the regenerated cartilage in the FGF10 group was densely stained by toluidine blue and by the anti-type II collagen antibody, but not by the anti-type I collagen antibody. The regenerated cartilage displayed a hyaline-like appearance with surface regularity and integration with the normal cartilage, whereas the defects in other groups still had not healed.

Histological Scores

The repaired tissue was assessed in a blinded manner by three observers using a modified version of Wakitani's grading scale. There were no significant differences in the scores obtained by the three observers (Fleiss' kappa score of total scores by the observers was 0.674). The histological scores of the FGF10 group improved continuously throughout the 24 weeks of the study, and the overall score of the FGF10 group across all time points was higher than those of all other groups (for each, $p < 0.05$; Fig. 6). Scoring rates in each category are shown in Table 2.

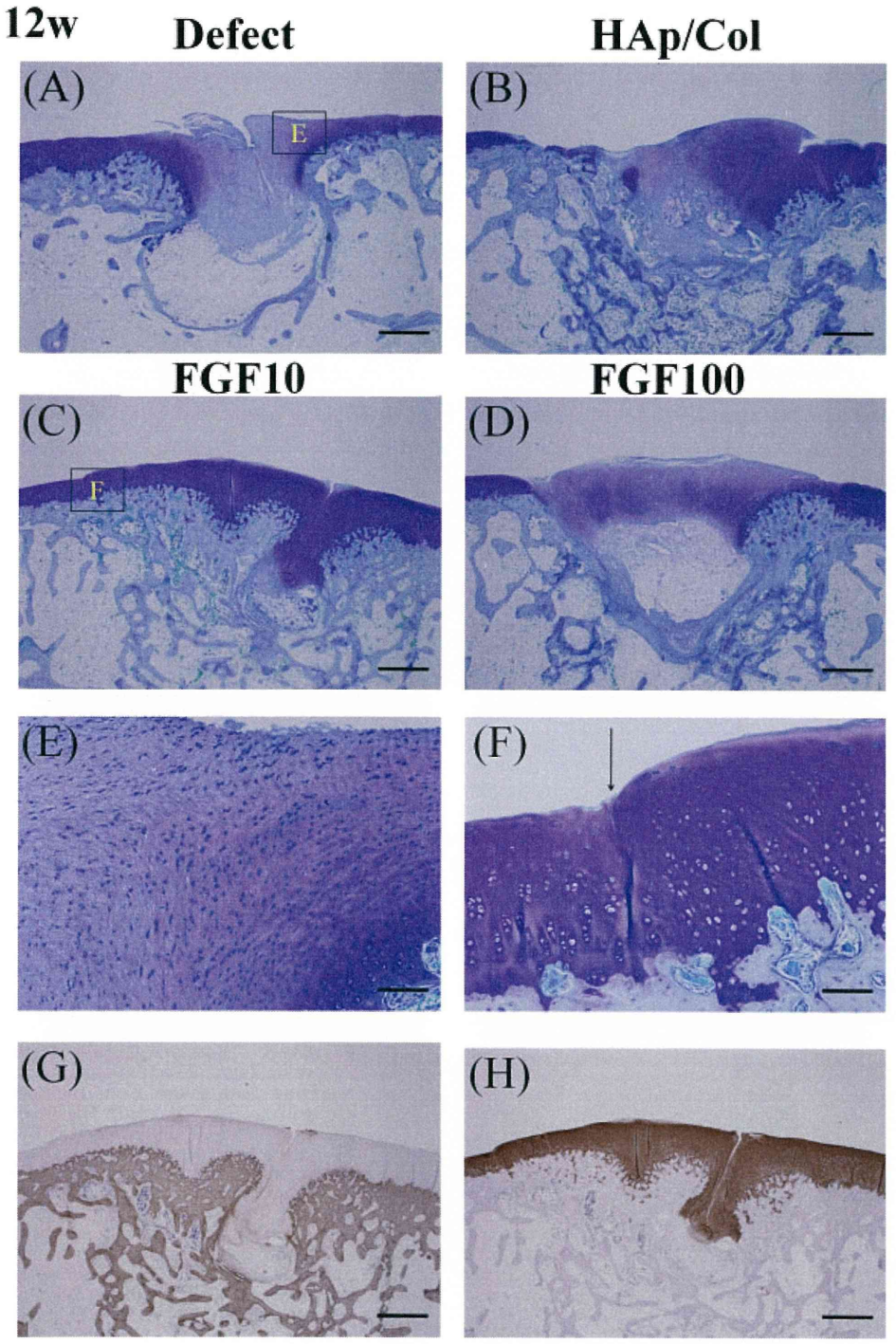

Figure 4. Histological observation at 12 weeks: Sagittal sections stained with toluidine blue taken from the defect group (A), HAp/Col group (B), FGF10 group (C), or FGF100 group (D). Panels (E) and (F) show the framed areas in panels (A) and (C) at higher magnification. The arrow in panel (F) indicates the boundary between newly formed cartilage and the surrounding native cartilage. Immunohistochemistry for type I (G) and type II (H) collagen in the regenerated tissue of the FGF10 group. Scale bars represent 1 mm for (A–D), (G) and (H), and 125 μm for (E) and (F).

DISCUSSION

This study investigated the effect of porous HAp/Col impregnated with FGF-2 on the restoration of large osteochondral defects in the rabbit model. Our results demonstrated the ability of porous HAp/Col in combination with a low dose of FGF-2 to repair osteochondral defects.

Regeneration of full-thickness cartilage defects is related to the size of the defect.[23,24] Smaller cylindrical full-thickness defects (3 mm) spontaneously regenerate articular cartilage. In contrast, larger defects (5 mm) result in the formation of fibrous scar tissue. This study established a new method for implanting porous HAp/Col impregnated with FGF-2 to repair the defect observed in a large (5 mm diameter) cylindrical full-thickness defect model.

Porous HAp/Col is a bone void filler that has high osteoconductivity, bioabsorbability, elasticity, and

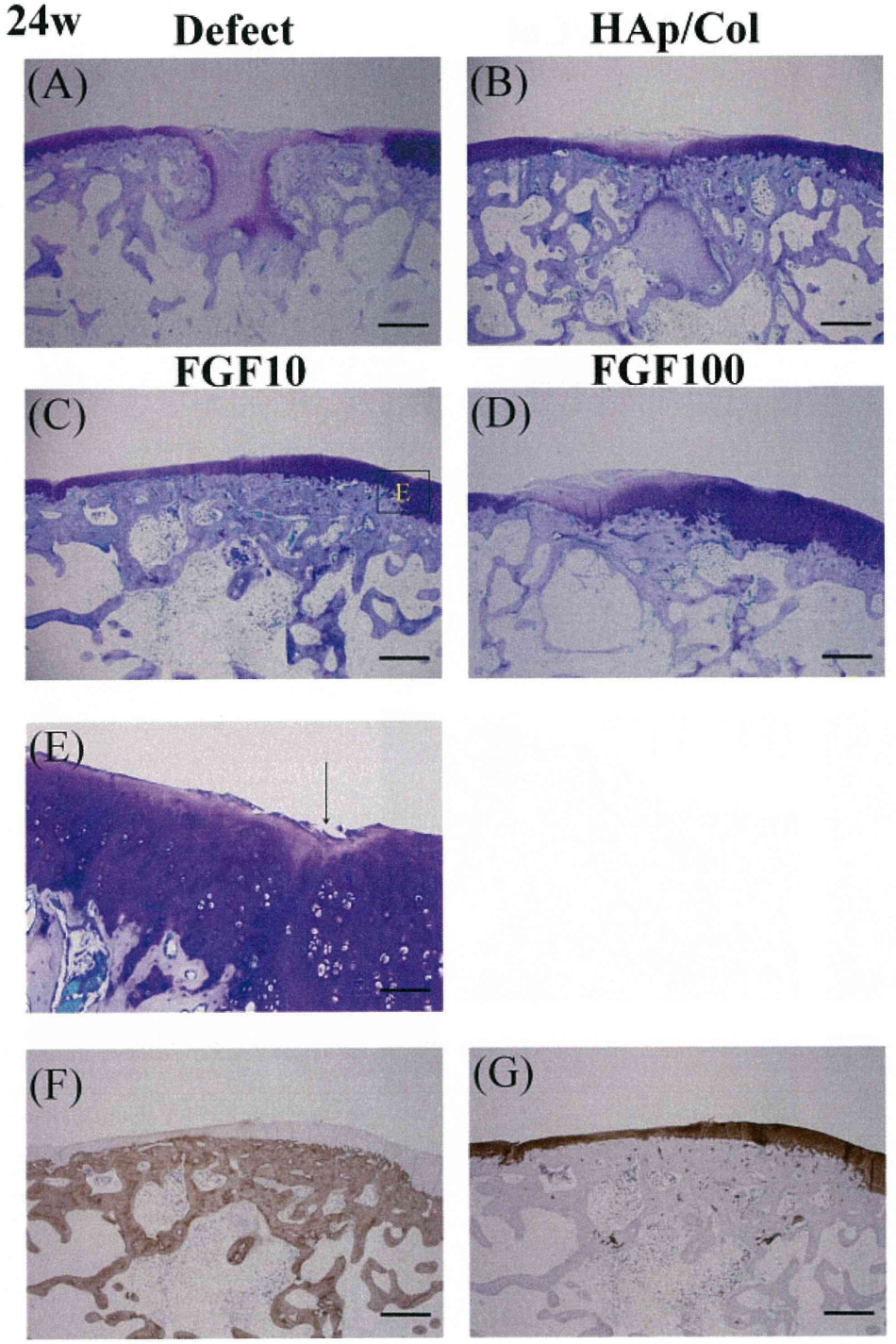

Figure 5. Histological observation at 24 weeks: Sagittal sections stained with toluidine blue taken from the defect group (A), HAp/Col group (B), FGF10 group (C), or FGF100 group (D). Panel (E) shows the framed area in panel (C) at higher magnification. The arrow in panel (E) indicates the boundary between newly formed cartilage and the surrounding native cartilage. Immunohistochemistry for type I (F) and type II (G) collagen in the repaired tissue of the FGF10 group. Scale bars represent 1 mm for (A–D), (F) and (G), and 125 μm for (E).

excellent handling. The material is highly porous (porosity: 95%), and the pore size (100–500 μm) is appropriate for bone formation. Due to these distinctive properties, we attempted to transplant the material into the subchondral bone level of the defect in order to promote bone repair. Bone formation was denser in the implanted HAp/Col groups than in the control group. The most abundant bone regeneration and the most satisfactory cartilage regeneration were obtained in the FGF10 group. According to previous reports[6,25] and, in accord with the correlation between cartilage repair and subchondral bone formation observed in our study, activation of the subchondral bone repair process probably enhanced the direct effects of FGF-2 on articular cartilage regeneration. Subchondral bone formation may have resulted from subchondral bone repair induced by the osteoconductive property of porous HAp/Col. Actively regenerating subchondral bone is likely to recruit additional pluripotent progenitor cells to the defect, demonstrating the concept of marrow

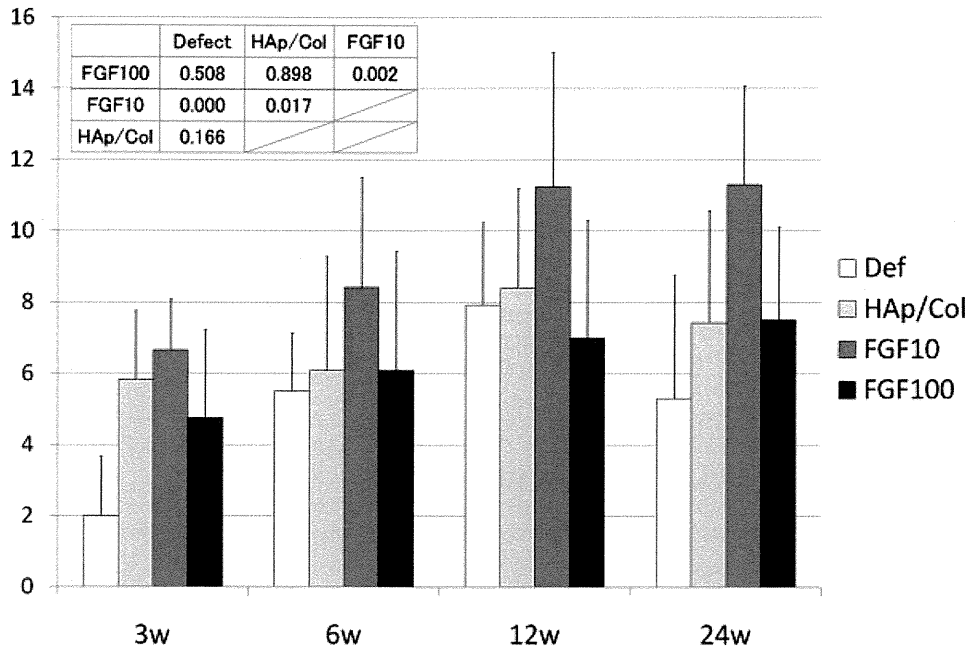

Figure 6. Histological scoring of the repaired tissue; histological findings were quantified using a scoring system (Table 1) where the score for normal cartilage was 16 points. The graph indicates mean values and standard deviations; *p*-values of overall scores across all time points between each group are shown in the panel included in the graph.

stimulation.[26,27] Alternately, factors secreted by actively regenerating cells in subchondral bone may exert paracrine effects on cartilage regeneration.

FGF-2 facilitates the synthesis of cartilaginous matrix by chondrocytes.[12,13] In the present study, although the basic HAp/Col transplant did not successfully result in full cartilage repair, HAp/Col impregnated with a low dose of FGF-2 promoted subchondral bone and cartilage regeneration. However, with a high-dose FGF-2, the regeneration of cartilage and its underlying subchondral area was poor. Biphasic dose-dependent responses are commonly observed in the context of growth factor biology.[28,29] High doses of FGF-2 may downregulate FGF receptors, reducing the growth factor's specific action. The FGF-2 doses used in this study were chosen based on previous reports.[14–16] There are some reports of successful osteochondral defect regeneration with a lower dose of FGF-2 than that used in our study.[30,31] The low-dose FGF-2 in our study demonstrated a superior improvement of osteochondral defect regeneration compared to the high-dose FGF-2. Lower-dose FGF-2 combined with porous HAp/Col, therefore, may be more effective for osteochondral regeneration.

Table 2. Scoring Rates in Each Category

		Scoring Rate (%) (SD)					
	Time (Weeks)	Cell Morphology	Matrix Staining	Surface Regularity	Thickness of Cartilage	Regenerated Subchondral Bone	Integration with Adjacent Cartilage
Defect	3	15.3 (12.3)	18.5 (16.7)	22.2 (17.2)	0.0 (0.0)	0.0 (0.0)	8.3 (20.4)
HAp/Col		30.6 (10.1)	37.0 (9.1)	42.6 (27.6)	13.9 (19.5)	47.2 (26.7)	47.2 (22.2)
FGF10		30.6 (10.1)	38.9 (13.6)	50.0 (18.3)	30.6 (24.5)	50.0 (0.0)	58.3 (20.4)
FGF100		30.6 (15.8)	25.0 (20.4)	38.9 (23.0)	8.3 (20.4)	52.8 (28.7)	30.6 (35.6)
Defect	6	33.3 (12.9)	33.3 (0.0)	51.9 (16.7)	16.7 (23.6)	13.9 (19.5)	44.4 (13.6)
HAp/Col		37.5 (13.7)	33.3 (21.1)	33.3 (29.8)	33.3 (25.8)	27.8 (25.1)	61.1 (25.1)
FGF10		50.0 (15.8)	50.0 (27.9)	44.4 (27.2)	50.0 (31.6)	66.7 (27.9)	63.9 (22.2)
FGF100		37.5 (13.7)	33.3 (21.1)	33.3 (29.8)	27.8 (25.1)	33.3 (40.8)	66.7 (25.8)
Defect	12	51.4 (16.2)	51.9 (16.7)	46.3 (16.4)	58.3 (18.6)	25.0 (23.0)	58.3 (20.4)
HAp/Col		43.3 (13.7)	40.0 (14.9)	60.0 (27.9)	50.0 (35.4)	56.7 (19.0)	76.7 (25.3)
FGF10		62.5 (20.9)	61.1 (25.1)	72.2 (32.8)	80.6 (24.5)	75.0 (27.4)	83.3 (25.8)
FGF100		48.3 (23.1)	44.4 (15.7)	33.3 (23.6)	43.3 (38.4)	30.0 (27.4)	60.0 (22.4)
Defect	24	31.7 (17.1)	33.3 (20.8)	33.3 (33.3)	30.0 (27.4)	30.0 (27.4)	36.7 (21.7)
HAp/Col		48.6 (14.4)	44.4 (17.2)	37.0 (21.8)	33.3 (40.8)	47.2 (26.7)	66.7 (38.0)
FGF10		65.0 (13.7)	60.0 (27.9)	71.1 (25.6)	70.0 (27.4)	90.0 (22.4)	80.0 (27.4)
FGF100		51.4 (12.3)	46.3 (16.4)	40.7 (19.5)	41.7 (20.4)	41.7 (34.6)	58.3 (20.4)

Our results also demonstrated the effectiveness of porous HAp/Col as an FGF-2 carrier. FGF 10 and 100 without HAp/Col groups were also tested although only three weeks post operatively. They did not show any improvement compared to the control at three weeks after the surgery. The release profile of FGF-2 from porous HAp/Col was also assessed. Although a precise release profile was not elucidated owing to rapid degeneration of FGF-2 dissolved in PBS, the assessment indicated that degeneration of FGF-2 adsorbed on HAp/Col was reduced compared to FGF-2 dissolved in PBS (data not shown) HAp/Col exhibits sponge-like hydrophilia, which are advantageous in a vehicle for drug delivery. Furthermore, because the HAp crystals contained in HAp/Col are on the nanoscale, porous HAp/Col has a high surface area, effectively promoting the absorption of molecules with an affinity for HAp, such as BMPs and TGF-β. Previous reports have demonstrated the usefulness of HAp/Col implants.[21,32,33] Some BMPs are known to facilitate cartilage regeneration,[5–7] preserve cartilage,[34,35] and promote chondrogenic differentiation of bone marrow stem cells.[36] Consequently, porous HAp/Col combined with BMPs in addition to FGF-2 may provide a means to repair osteochondral defects more successfully.

Prior to clinical application, further studies, including evaluation of the mechanical properties of regenerated cartilage, will be required to determine the optimal dose of FGF-2, the advisability of combination with other drugs, the particularities of various defect sizes, and the responses of different animals. Depending on the results of these studies, it may be possible to develop acellular treatments for chondral and osteochondral defects by using the porous HAp/Col as a scaffold and as a carrier for drug delivery.

In conclusion, we have successfully induced repair of large full-thickness osteochondral defects in a rabbit model using porous HAp/Col as a scaffold and a carrier for FGF-2, although further study is required to determine the optimal dose of FGF-2.

ACKNOWLEDGMENTS

This work was supported by a Grant-in-Aid for Scientific Research from the Ministry of Education, Culture, Sports, Science and Technology of Japan.

REFERENCES

1. Mandelbaum BR, Browne JE, Freddie F. 1998. Articular cartilage lesions of the knee. Am J Sports Med 26:853–861.
2. Shapiro F, Koide S, Glimcher MJ. 1993. Cell origin and differentiation in the repair of full-thickness defects of articular cartilage. J Bone Joint Surg [Am] 75-A:532–553.
3. Smith GD, Knutsen G, Richardson JB. 2005. A clinical review of cartilage repair techniques. J Bone Joint Surg [Br] 87-B: 445–449.
4. Fujisato T, Sajiki T, Liu Q, et al. 1996. Effect of basic fibroblast growth factor on cartilage regeneration in chondrocyte-seeded collagen sponge scaffold. Biomaterials 17:155–162.
5. Sellers RS, Peluso D, Morris EA. 1997. The effect of recombinant human bone morphogenetic protein-2 (rhBMP-2) on the healing of full-thickness defects of articular cartilage. J Bone Joint Surg [Am] 79:1452–1463.
6. Tamai N, Myoui A, Hirao M, et al. 2005. A new biotechnology for articular cartilage repair: subchondral implantation of a composite of interconnected porous hydroxyapatite, synthetic polymer (PLA-PEG), and bone morphogenetic protein-2 (rhBMP-2). Osteoarthritis Cartilage 13:405–417.
7. Cook SD, Patron LP, Salkeld SL, et al. 2003. Repair of articular cartilage defects with osteogenic protein-1(BMP-7) in dogs. J Bone Joint Surg [Am] 85-A(Suppl 3):116–123.
8. Holland TA, Bodde EW, Baggett LS, et al. 2005. Osteochondral repair in the rabbit model utilizing bilayered, degradable oligo(poly(ethylene glycol) fumarate) hydrogel scaffolds. J Biomed Mater Res A 75:156–167.
9. Wakitani S, Imoto K, Kimura T, et al. 1997. Hepatocyte growth factor facilitates cartilage repair. Full thickness articular cartilage defect studied in rabbit knees. Acta Orthop Scand 68:474–480.
10. Froger-Gaillard B, Charrier AM, Thenet S, et al. 1989. Growth-promoting effects of acidic and basic fibroblast growth factor on rabbit articular chondrocytes aging in culture. Exp Cell Res 183:388.
11. Gonzalez AM, Buscaglia M, Ong M, et al. 1990. Distribution of basic fibroblast growth factor in the 18-day rat fetus: localization in the basement membranes of diverse tissues. J Cell Biol 110:753–765.
12. Nimni ME. 1997. Polypeptide growth factors: targeted delivery systems. Biomaterials 18:1201–1225.
13. Kato Y, Iwamoto M, Koike T. 1987. Fibroblast growth factor stimulates colony formation of differentiated chondrocytes in soft agar. J Cell Physiol 133:491–498.
14. Fukuda A, Kato K, Masahiro H, et al. 2005. Enhanced repair of large osteochondral defects using a combination of artificial cartilage and basic fibroblast growth factor. Biomaterials 26: 4301–4308.
15. Fujimoto E, Ochi M, Kato Y, et al. 1999. Beneficial effect of basic fibroblast growth factor on the repair of full-thickness defects in rabbit articular cartilage. Arch Orthop Trauma Surg 119:139–145.
16. Miyakoshi N, Kobayashi M, Nozaka K, et al. 2005. Effects of intraarticular administration of basic fibroblast growth factor with hyaluronic acid on osteochondral defects of the knee in rabbits. Arch Orthop Trauma Surg 125:683–692.
17. Kikuchi M, Itoh S, Ichinose S, et al. 2001. Self-organization mechanism in a bone-like hydroxyapatite/collagen nanocomposite synthesized in vitro and its biological reaction in vivo. Biomaterials 22:1705–1711.
18. Rhee SH, Suetsugu Y, Tanaka J. 2001. Biomimetic configurational arrays of hydroxyapatite nanocrystals on bio-organics. Biomaterials 22:2843–2847.
19. Kikuchi M, Ikoma T, Syoji D, et al. 2004. Porous body preparation of hydroxyapatite/collagen nanocomposites for bone tissue regeneration. Key Eng Mater 254:561–564.
20. Yunoki S, Ikoma T, Tsuchiya A, et al. 2007. Fabrication and mechanical and tissue ingrowth properties of unidirectionally porous hydroxyapatite/collage composite. J Biomed Mater Res B Appl Biomater 80:166–173.
21. Sotome S, Orii H, Kikuchi M, et al. 2006. In vivo evaluation of porous hydroxyapatite/collagen composite as a carrier of OP-1 in a rabbit PLF model. Key Eng Mater 309-311:977–980.
22. Wakitani S, Goto T, Pineda SJ, et al. 1994. Mesenchymal cell-based repair of large, full-thickness defects of articular cartilage. J Bone Joint Surg [Am] 76:579–592.
23. Mizuta H, Kudo S, Nakamura E, et al. 2004. Active proliferation of mesenchymal cells prior to the chondrogenic repair response in rabbit full-thickness defects of articular cartilage. Osteoarthritis Cartilage 12:586–596.